Long Term Degradation of Resin for High Temperature Composites

Kaustubh A. Patekar
Massachusetts Institute of Technology, Cambridge, Massachusetts

Since its founding, NASA has been dedicated to the advancement of aeronautics and space science. The NASA Scientific and Technical Information (STI) Program Office plays a key part in helping NASA maintain this important role.

The NASA STI Program Office is operated by Langley Research Center, the Lead Center for NASA's scientific and technical information. The NASA STI Program Office provides access to the NASA STI Database, the largest collection of aeronautical and space science STI in the world. The Program Office is also NASA's institutional mechanism for disseminating the results of its research and development activities. These results are published by NASA in the NASA STI Report Series, which includes the following report types:

- TECHNICAL PUBLICATION. Reports of completed research or a major significant phase of research that present the results of NASA programs and include extensive data or theoretical analysis. Includes compilations of significant scientific and technical data and information deemed to be of continuing reference value. NASA's counterpart of peer-reviewed formal professional papers but has less stringent limitations on manuscript length and extent of graphic presentations.

- TECHNICAL MEMORANDUM. Scientific and technical findings that are preliminary or of specialized interest, e.g., quick release reports, working papers, and bibliographies that contain minimal annotation. Does not contain extensive analysis.

- CONTRACTOR REPORT. Scientific and technical findings by NASA-sponsored contractors and grantees.

- CONFERENCE PUBLICATION. Collected papers from scientific and technical conferences, symposia, seminars, or other meetings sponsored or cosponsored by NASA.

- SPECIAL PUBLICATION. Scientific, technical, or historical information from NASA programs, projects, and missions, often concerned with subjects having substantial public interest.

- TECHNICAL TRANSLATION. English-language translations of foreign scientific and technical material pertinent to NASA's mission.

Specialized services that complement the STI Program Office's diverse offerings include creating custom thesauri, building customized data bases, organizing and publishing research results . . . even providing videos.

For more information about the NASA STI Program Office, see the following:

- Access the NASA STI Program Home Page at *http://www.sti.nasa.gov*

- E-mail your question via the Internet to help@sti.nasa.gov

- Fax your question to the NASA Access Help Desk at (301) 621-0134

- Telephone the NASA Access Help Desk at (301) 621-0390

- Write to:
  NASA Access Help Desk
  NASA Center for AeroSpace Information
  7121 Standard Drive
  Hanover, MD 21076

NASA/CR—2000-209918

Long Term Degradation of Resin for High Temperature Composites

Kaustubh A. Patekar
Massachusetts Institute of Technology, Cambridge, Massachusetts

National Aeronautics and
Space Administration

Glenn Research Center

February 2000

Acknowledgments

A number of people contributed in various ways towards this endeavor. First of all, I would like to thank Hugh, my advisor, for his guidance and encouragement. I have enjoyed working for him. The discussions I had with him helped form the basis of this work and his suggestions were instrumental in making my life a lot easier. I would also like to thank Paul, Mark, Carlos and Prof. Dugundji for their comments and questions during TELAC presentations. The discussion on issues raised during these talks helped to improve the quality of this work. John Kane's help in getting my long-lasting tests done is greatly appreciated. Deb, thank you for keeping me company while waiting for Hugh and enduring my "Where is Hugh?" questions, especially during the last two months. Thanks Ping for decoding all those requisition forms. Thanks are due to my UROPers Jeff Reichbach and Ryan Peoples, for going through numerous catalogs and building the experimental set-up. I owe a lot to other grad students in the lab, who have made this time fly by. Chris, for keeping me company while working at ungodly hours in the office (I have never seen him leave for the day). Tom, for being nice and letting me use the thermal chamber for a really long time. Lauren, Brian and Dennis for all those chats, which were good, relaxing breaks. All those who have offices in 41-219, for sharing the joy of working in a place that continues to oscillate between the equator and Antarctica.

FOREWORD

TABLE OF CONTENTS

LIST OF FIGURES

LIST OF TABLES

NOMENCLATURE

c_{ox} relative concentration of oxygen

c_s relative concentration of species s

C_i constant used for modeling reaction during data reduction

E_i activation energy of reaction acting on component i

E_{ij} activation energy of reaction j acting on component i

$F'(T)$ temperature-dependence function

$F(\alpha_i)$ conversion-dependence function for component i

k_i rate constant for reaction acting on component i

k_{ij} rate constant for reaction j acting on component i

m_f final mass of unreacting mass fractions

m_i mass lost due to completion of reactions on component i

m_{ij} concentration-dependency of reaction j acting on component i

m_o original mass of material in an infinitesimal control volume

m_{si} concentration-dependency of reaction acting on species s

m_{fi} final mass of component i

m_{oi} original mass of component i

n_i order of reaction acting on component i

n_{ij} order of reaction i acting on component i

M_0 original sample mass for experiments

$M(t)$ sample mass measured at time t

R real gas constant

t time

T absolute temperature

V specimen volume

y_i mass fraction of component i

α_i mass loss metric for component i

α_{ij} mass loss metric for reaction j acting on component i

Δm total mass lost from control volume

Δm_n normalized mass loss for sample used in tests

$\Delta m'$ normalized mass lost from control volume

Δm_i mass lost from component i

ΔM total mass lost from volume V

CHAPTER 1

INTRODUCTION

Polymer matrix composites are being increasingly used in applications where they are exposed to harsh environmental conditions such as high temperatures, thermal cycling, moisture, gases, oils and solvents. Exposure to such environments leads to degradation of composite materials, potentially affecting the structural integrity and useful lifetimes of composite structures. Some of the well-known aerospace applications of polymer matrix composites (PMCs) include engine supports and cowlings, reusable launch vehicle parts, radomes, thrust-vectoring flaps and thermal insulation of rocket motors.

The increasing demand for such applications has led to extensive efforts for the development of materials which have upper use temperatures in excess of 150°C. These materials should be able to withstand a wide range of temperatures without significant reduction in their mechanical properties, be chemically resistant to the environment and exhibit low mass loss at extended aging times at their upper use temperatures.

The behavior of PMCs exposed to high temperatures for extended durations is not well understood. A variety of effects are observed on matrix materials, including specimen mass loss, specimen shrinkage, the development of a severely degraded surface layer, formation of voids, the development of surface microcracks, and the degradation of mechanical properties. The problem is further complicated by the anistropic nature of composite materials. The fiber/matrix interface provides additional sites for

both degradation and the formation of cracks. Composite laminates also experience thermally (or mechanically) induced interply microcracks in the matrix material. These cracks can then provide new pathways into the interior of the material for the external environment, resulting in more severe degradation of the laminate as a whole. The interaction of these effects during the aging period results in a highly complex, coupled problem where the identification of individual mechanisms and their contributions becomes extremely difficult.

As noted by Cunningham [1], design of high temperature structures would be greatly improved through the development of a model which could incorporate known quantities such as laminate geometry, material properties, temperatures and chemical environment, and from these determine quantities such as the material degradation state as functions of exposure time and position within the material. A schematic of the desired coupled analysis which could provide this capacity is shown in Figure 1.1. The analysis consists of several individual modules which address different aspects of the problem. Inputs to the model include the exposure environment and the applied mechanical loads. For a comprehensive analysis, it is necessary to calculate the thermal response, diffusion and chemical degradation state, and the thermo-mechanical response of the system. The thermal analysis supplies the diffusion and reaction chemistry model with the necessary temperatures. This module can then provide the thermo-mechanical analysis with predictions of the chemical state within the material. Results from these analyses can then be used to determine whether damage (and ultimately failure) occurs. The effects of damage on material properties, thermal response and the reaction chemistry is accounted for in an incremental fashion, allowing a truly coupled

2
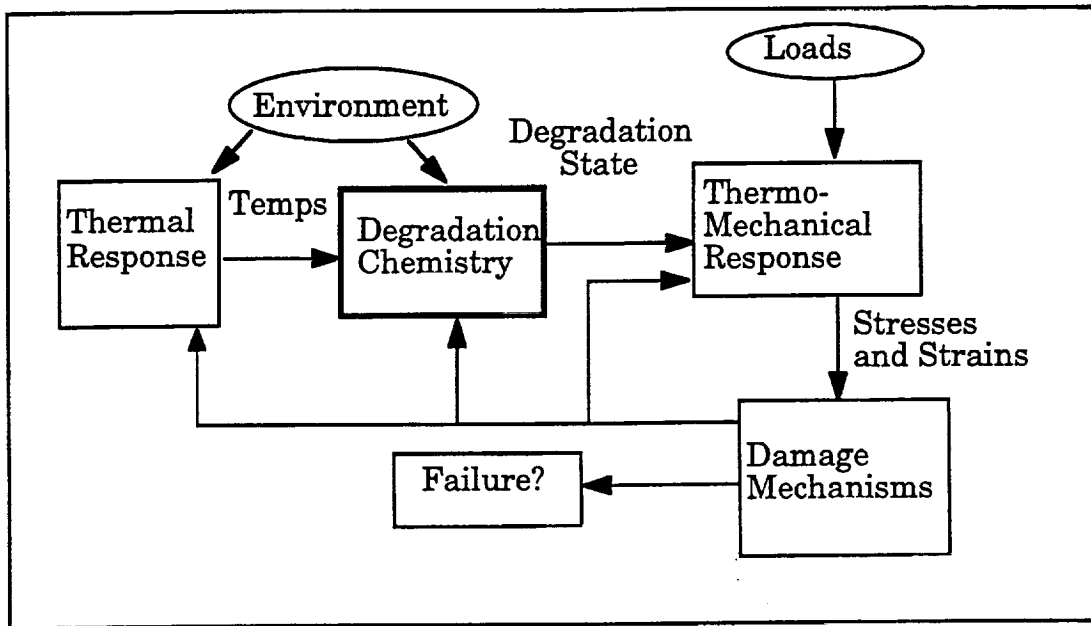
Figure 1.1   Complete analysis for composite degradation

representation of the problem. Though substantial success has been achieved in solving different sections of this complex problem, the chemical degradation has not been adequately quantified.

The current research uses, and hopes to validate, a mass loss (or gain) metric for the chemical degradation within a polymer matrix composite material. The extent to which such a metric can be used for developing predictive capability, assuming that the time and nature of environmental exposure of a composite are known, is studied. The approach found to be useful by other researchers [1],[2] consists of using Arrhenius reaction kinetics to model chemical reactions which occur within the material. Two types of reactions are considered: thermal reactions which depend primarily on the duration and temperature of exposure, and oxidative reactions which also take into account the exposure to oxygen.

The goal of the current research is to establish an analytical methodology which can be used to predict the degradation states at all points within a composite laminate as functions of exposure time and environment. The analysis uses Arrhenius reaction kinetics to model the chemical reactions which occur within the material. Multiple, simultaneously occurring chemical reactions, including both purely thermal reactions and reactions that depend on diffusing substances, are taken into account. Some of the earlier work, which formed the basis for this work, showed that the concentration of diffusing oxygen controls some of the chemical reactions. In this work we studied only powdered matrix materials so as to decouple the diffusion effects from the chemical effects. A better understanding is currently needed of these chemical effects.

Experimental studies were carried out to characterize the nature of chemical reactions, and to determine appropriate models and to quantify

4

them with kinetic reaction coefficients. Long term isothermal tests for duration in excess of 200 hours were carried out on finely ground neat resin powders in both thermal and oxidative environments. The use of fine powders, which have very large surface area to volume ratios, effectively eliminates the diffusion effects which can be seen in finite-sized specimens [3]. Mass losses were measured for tests carried out at different temperatures and this data was used to obtain the required chemical reaction coefficients for the model.

Some of the earlier work had utilized thermogravimetric analyses (TGAs) for measuring the mass loss and mass loss rate on powdered samples. However, this technique was found to be very expensive for conducting long term isothermal tests. A new cost-effective technique was developed for conducting these tests. This technique makes use of an oven with a temperature controller, a custom setup for holding the sample, and a sensitive weighing balance to measure the sample mass periodically.

Previous work relevant to the current research and some of the research which led to this work are described in Chapter 2. This includes analytical and experimental studies on the degradation of high temperature PMCs as well as a background on the analytical chemistry used in the course of this work. The problem statement and approach for the current research is presented in Chapter 3. The analytical methodology is developed in Chapter 4. Chapter 5 describes the experimental procedure that was developed to collect data for predicting required material coefficients. Experimental results, as well as correlation between experimental data and model predictions is presented and discussed in Chapter 6. Finally, conclusions reached on the basis of this work are presented in Chapter 7.

CHAPTER 2

BACKGROUND

A number of polymer matrix composites are being used in the aerospace industry for high temperature applications. Most of these materials are thermosetting resins which can be chemically classified as bismaleimides and polyimides. These resins have proven to be better than traditional polymer systems in terms of chemical resistance, ability to withstand high temperatures, and maintaining structural strength and integrity. However, documenting the behavior of these materials has clearly shown that these materials degrade with continued exposure to high temperatures. The durability issues related to these materials need to be well understood in order to use them with confidence in primary structure applications and to improve the design of aerospace components where they are currently being used.

Introduced in the early 1970s by researchers at NASA Lewis Research Center, PMR-15 and other polyimides are among the most widely used in high temperature applications. These materials exhibit the required mechanical properties and thermo-oxidative stability [4], [5], [6]. While PMR-15 has been used in continuous service at 500 to 550F, some of the next-generation materials withstand continuous service of 600 to 700F with excursions to 800F and beyond.

Most of the experimental work carried out to improve the understanding of these materials has focused on the collection of experimental data, with the idea of creating a database of the effects of

extended exposure to high temperatures. Some of the recent work has tried to build empirical modes for correlating the degradation effects with changes in material properties such as strength and weight. There is only a small amount of work which has tried to quantify the phenomena with the aim of building accurate analytical models.

Most of the analytical work has led to the building of case-specific quantitative models and only a very limited number of mechanism-based models [1], [7]. These mechanism-based models were successful in capturing some of the degradation phenomena. However more work is needed for developing predictive capability based on these mechanism-based high temperature degradation models.

Some of the relevant experimental studies and analytical work is reviewed in this chapter. Studies in the area of polymer chemistry are discussed in order to give adequate background for this work, which focuses on quantifying the reaction mechanisms.

2.1   PREVIOUS EXPERIMENTAL STUDIES

The extensive experimental data on high temperature degradation can be broadly classified into three categories - effects of aging on neat resin [8], [9], bare fibers [10], [11], [12], [13] and composite materials [4], [14], [15], [16]. Mass loss, shrinkage, and changes in thermal, mechanical and viscoelastic behavior have been reported. Limited correlation exists between individual studies.

A study by Bowles [9] on the effects of aging on neat PMR-15 resin revealed that several coupled mechanisms proceed simultaneously in the early stages of degradation at elevated temperatures in air. Samples exposed for up to 3000 hours at temperatures ranging between 288°C and 343°C

exhibited mass loss, specimen shrinkage, the formation of a distinct surface layer, development of surface microcracks, and the degradation of mechanical properties. Mass loss occurs throughout the duration of the aging periods observed, and in the presence of oxygen results in the formation of a distinctive thin layer on the exposed surfaces of the polymer. Voids develop within the surface layer and increase in size and density over time, acting as starter points for cracks which grow from the exposed surfaces. The similarity between the observed surface layer growth rates and mass loss rates suggests that degradation-induced mass loss primarily occurs within this thin surface layer, while the core of the material is relatively protected from oxidative degradation. This suggests that diffusion of environment into the material plays a key role and is coupled with the chemical degradation phenomenon.

Similar investigations on the effects of aging at elevated temperatures on bare fibers have also been conducted. Bowles [12] found that extended exposure in air resulted in mass loss from graphite fibers. Data from this study suggested that carbon fibers such as Celion 6000 consist of a layered microstructure which has a relatively non-porous outer skin surrounding a porous core. As the outer layer degrades the environment gains access to the inner, porous core, resulting in an acceleration of the degradation process. This effect was also noted by Wong *et al.* [13] in a study on the thermo-oxidative stability of IM6 fibers in air. In contrast, fibers in composites are protected – virtually no surface area is exposed to the environment and no mass loss is observed [11]. This suggests that adequate quantification of the matrix degradation is important for studying composite behavior at high temperatures as the fibers will not be exposed to environment in most cases where such materials are used.

Unidirectional composites demonstrate similar degradation mechanisms to neat resin, although the mass loss is less severe. Mass loss appears to be dependent on the matrix volume fraction [14], suggesting that preferential degradation of the matrix takes place. A study on the effects of different aging environments on the mass loss from unidirectional graphite-fiber/PMR-15 composites recorded significant differences in the mass loss behavior in inert and oxidative atmospheres [4]. Mass losses in inert atmospheres asymptotically approached stable values over a period of time at each of the test temperatures. The majority of the mass loss occurs within the first few hundred hours of aging and appears to be a bulk mechanism, depending only on specimen volume. After the first 150 hours of aging, mass losses from the specimens at each of the aging temperatures have essentially reached their final values, which increases with exposure temperature. This behavior suggests that only the initial portion of the mass loss curves reflect thermally activated processes. In contrast, specimens exposed to oxidative atmospheres will continually lose mass over the entire aging period. Notably higher mass loss rates are demonstrated in air than in an inert atmosphere at the same temperature. Aging in oxidative atmospheres always results in the formation of degraded surface layers. As aging time is increased, a distinct layer of degraded matrix forms at the surfaces and advances into the composite [15]. This layer growth is similar to that observed in neat resin [9]. Scola and Vontell [16] measured the flexural and shear properties of graphite fiber/PMR-15 composites, isothermally aged at 316°C for periods up to 2000 hours, for a number of different fibers. SEM analysis of fractured surfaces was carried out and optical micrographs of cross-sections were taken. They observed that composites with high initial shear strength exhibited the greatest resistance to reduction in shear strength. They did not hypothesize

the possible cause of this behavior. These data seem to suggest that the fiber/matrix interaction played a role in the degradation of the composite shear strength.

The influence of the fiber reinforcements on thermo-oxidative stability has been addressed by several research efforts [10], [11], [14] in trying to explain the accelerating effect of exposed graphite fiber ends on mass loss rates in composites. These researchers recorded different behavior in composite materials with different fiber reinforcements. The mass loss behavior was blamed on the effects of impurities in fibers; which in turn allowed fiber degradation, exposing greater matrix surface are to degradation. The most thermally stable fibers do not necessarily result in the most stable composites, and in some cases result in the least thermo-oxidatively stable configurations [12].

2.2 POLYIMIDE CHEMISTRY

The degradation behavior which has been observed empirically is dependent primarily upon the chemistry of the matrix material. The PMR-15 material considered in the course of this work is chemically quite complex. PMR polyimides are addition-type thermosetting polymers prepared by the polymerization of monomer reactants (PMR). Resin solutions consist of three individual monomers - a nadic ester (NE), the dimethyl ester of 3,3',4,4'-benzophenotetracarboxylic acid (BTDE), and 4,4'-methylenedianiline (MDA) dissolved in methanol. When these monomers are combined in a 2.000/2.087/3.087 molar ratio respectively, the formulated weight after imidization, but before crosslinking, is 1500. Resin of this composition is designated PMR-15 [17] . The chemistry of the formation of this building block is quite well understood [18] , however the chemistry involved in the

11

polymerization and later cross-linking of the material is still subject to much debate with no definitive answer as yet available [8], [19]. The chemistry involved in the degradation of this and other related systems is under investigation but it is not yet understood to a level which would allow definite conclusions to be drawn and predictive calculations to be made.

Evidence suggests that cross-linking within the material is not complete at the end of the post-cure period, and hence one aspect of the aging process is the completion of cross-linking reactions. Studies have linked this increase in cross-link density within the material to the initial increase in material properties such as the glass transition temperature and compressive modulus [2], [20].

The fully cross-linked material is subject to both oxidative attack and thermal degradation at a variety of sites, both in the cross-links and in the main polymer chain itself at a variety of vulnerable links [21]. The mass loss over extended aging times is attributed to the degradation of the nadic ester and MDA components of the main polymer chain while the BTDE component remains relatively unaffected [22]. The nadic ester appears to be the most vulnerable to oxidative attack and is thus the weak link in the thermo-oxidative stability of these materials, with an increase in the nadic ester content in the PMR formulation resulting in a decrease in the thermo-oxidative stability of the compound [23]. PMR formulations using the MDA component demonstrated lower mass loss and higher material property retention than PMRs formulated using more a stable monomer in place of MDA. This effect has been attributed to a synergy between the MDA/NE components which provides sites vulnerable to oxidation in the PMR polymer chain. These sites promote weight-gaining reactions (such as carbonyl formation and thermo-oxidative cross-linking) in surfaces exposed to air,

resulting in the polymer possessing a higher thermo-oxidative stability as a whole [21].

PMR-II-50, also developed at NASA is formulated with a hexafluoro-dianhydride (the diester thereof, 6FDE) instead of BTDE, for increased thermo-oxidative stability in the prepolymer backbone, and para-phenylenediamine (PPDA), replacing MDA. Prepolymer molecular weight is higher at 5000. This results in a 50 to 100F increase in the thermal stability, with some sacrifice in glass transition temperature due to cross-linking [5].

A great deal of mechanistic information concerning polyimidie degradation has been ascertained from analysis of the degradation products, both volatile off-gases and solid residues. The most prevalent products evolved during thermolysis of a polyimide are CO_2, CO and H_2O. At temperatures below about 350°C, CO_2 is the predominant gaseous by-product. Above 350°C, CO evolution commences and becomes pre-dominant above 400°C. The compositions of the volatile degradation products produced in air and nitrogen are qualitatively similar although rates of their formation are much greater in air [24]. Releases of larger fragments of the polymer may follow. In an inert atmosphere such as nitrogen, approximately 60% of the initial mass of the polymer will remain as char up to 800°C. In air, the more aggressive nature of the environment results in all of the mass being eventually consumed at these temperatures [25]. While the basic theory behind the chemistry of this degradation behavior is currently receiving considerable attention, the efforts in this area to develop a more complete understanding of this phenomenon remain too diverse to allow the development of a definitive model of the mechanisms which occur. A more focused research effort is required for achieving this goal.

2.3 PREVIOUS ANALYTICAL WORK

The confounded nature of experimental data due to the coupling of various physical effects, and the complex nature of PMR-15 chemistry, suggest the use of semi-empirical methods for modeling the degradation behavior. Various physical effects (e.g. diffusion vs. chemical reactions) can be studied by planning a careful set of experiments that decouple the physical effects. The chemistry has proven more difficult. Reasonable modeling success could be achieved, without a complete understanding of the underlying chemistry, if a metric can be developed for quantifying the degradation.

Attempts have been made to analyze and model various aspects of this problem. Mass loss rates have been empirically fit to Arrhenius rate curves [3]. Arrhenius rate kinetics represent an important, established method of reporting and comparing kinetic data. The Arrhenius rate equation expresses material conversion/degradation rate as a function of both temperature and conversion state. The true versatility of this model lies in the generality of the conversion-dependence function used in the rate equation, allowing a large variety of experimental rate measurements to be modeled in this manner [1]. This type of approach provides a simple means to model the stability of different systems but is useful only for comparative purposes if data is not collected and reduced in a rigorous manner. Other degradation models such as Coats/Redfern, Ingraham/Marier, and Horowitz/Metzger have also been fit to mass loss rate data [25]. These models are less general than the Arrhenius form, placing specific assumptions on the mechanisms which are being modeled. As such they are less versatile than the Arrhenius approach and are more commonly used as methods for comparing the stability of similar polymer systems subjected to

isothermal exposures than for determining kinetic parameters for predictive modeling.

More sophisticated models have combined modeling of the diffusion of oxygen into the material with chemical reaction rate equations to predict the mass loss and growth of degraded surface layers. In many such cases effective diffusion coefficient models are used [26] where an apparent diffusivity is found by fitting to experimental mass loss curves for a composite. Models of this kind allow the anisotropic nature of the degradation to be simulated but offer little insight to the true physics of the problem, effectively smearing many possible mechanisms together into the observed global effects.

Hinkley and Nelson [27] conducted tests on unidirectional LaRC™-160 and PMR-15 graphite composite for up to 25,000 hours. They used Arrhenius plots as empirical fits to obtain ranges of activation energy in a temperature band of 160-180°C. They were able to obtain reasonable lifetime extrapolations but did not succeed in capturing the underlying degradation mechanisms.

Nam and Seferis [28] developed a generalized methodology for composite degradation based on two elementary reaction mechanisms, hence allowing for both reaction and diffusion controlled degradation mechanisms. Several independent reaction mechanisms may be accounted for through the use of weighting factors. These weighting factors assign certain proportions of the overall mass loss to individual reactions, each with its own set of kinetic parameters, and thus allow a variety of complex chemical degradation processes to be modeled.

2.4 RECENT WORK

Most of the tests of this material exposed to a high temperature oxidative environment are difficult to interpret because of the coupled nature of the various degradation mechanisms and the non-uniformity of degradation. Tests are accelerated using temperatures and/or pressures higher than test conditions. However, the scaling factors associated with such tests are not well understood. It is not clear, for example, that diffusion and/or different chemical reactions will scale with temperature in the same way.

Models which can calculate [29] degraded composite laminate properties and behaviors based on known degradation states within the material have been developed. However, these models require accurate degradation and diffusion information, and require careful verification at all levels before they will be useful for predictive calculations.

The understanding of diffusion has substantially improved in the light of recent work. Cunningham [1] recorded the formation of degraded surface layers as functions of exposure time using photomicrographs at different temperatures. Geometry effects in the neat resin, and anistropic diffusion effects in the composites, were identified using specimens with different aspect ratios. The diffusion coefficients were calculated using this data.

The chemical degradation, though well understood, has not been accurately quantified due to the complex degradation chemistry of PMR-15. Thermogravimetric analyses (TGAs) were conducted on powdered specimens in nitrogen and air to separate the thermal reactions from the oxidative reactions. Tests were also carried out in oxygen to understand the effects of oxygen concentration on the degradation process. All these tests were carried out on powdered specimens to decouple the diffusion effects from the

chemical effects.

This work suggested that thermal reactions are made up of a spread of a large number of low mass fraction reactions, although the behavior at higher temperatures can be approximated using two effective Arrhenius reactions. These reactions die out rapidly as the temperature is lowered towards the use condition and so it may not be necessary to capture the behavior of these reactions with great accuracy.

Oxidative reactions are extremely active at test temperatures, and are also of concern at use temperatures. These reactions are concentration dependent and appear to consist of multiple reactions which have different rate and concentration dependencies. The confounded nature of these reactions makes it difficult to quantify the mass fractions on which they act. These reactions dominate the low temperature behavior and so an accurate representation of their behavior is needed. Cunningham [1] used high rate dynamic TGA tests to extract a preliminary set of modeled chemical reactions, but accuracy was limited, and extrapolation to use conditions was found to be unfeasible. The use of a test program that used large number of isothermal TGAs along with very low rate (below 1°C. min.) dynamic heating tests was recommended.

Isothermal TGAs on powdered specimens in nitrogen, air and oxygen [30] yielded activation energies in air which were approximately one-half of those in nitrogen, indicating that significantly less energy is required for oxidation as opposed to thermal degradation. Comparison between tests in air and oxygen have revealed a strong effect of relative oxygen concentration on reaction rate, with rates being greatly accelerated with increasing oxygen concentration. However, only comparative data was detailed in this study, data was not reduced to a set of kinetic coefficients which could be used in

analytical models.

Another way of attacking this problem is the simultaneous use of two or more techniques focused on studying the chemical phenomena. Liau *et al* [31] studied a organic polymer resin called Poly(Vinyl Butyral). Weight loss curves were fitted to an Arrhenius type equation and each reaction was identified from its major evolving gas. The amount of gases evolved were measured using Fourier Transform Infrared Spectrometry (FTIR). However, data from FTIR will be difficult to interpret in the case of polymers like PMR-15, in which multiple reactions lead to the formation of the same byproducts such as CO_2, CO and H_2O.

Jordan and Iroh [32] used gravimetry, differential scanning calorimetry (DSC) and FTIR to study the isothermal aging of partially imidized LaRC-IA polyimide resin. Qualitative information can be obtained from spectral assignment of intermediate and final reaction products, while quantitative evaluation of the spectra recorded in a predetermined time interval provides the basis for the determination of reaction kinetics. The time dependent intensity changes, measured at different temperatures provide the data used to determine the reaction kinetics. The authors collected the relevant data but did not demonstrate its use for obtaining the reaction constants.

Another factor left untouched in most of the other work is the effect of fabrication parameters on the degradation process. Weisshaus and Engleberg [33] studied ablative composites used as thermal active insulation used in rocket nozzles. They measured failure mode and tensile strength at temperatures from ambient to 900°C for samples which had been manufactured by the same process, but with different levels of forming pressure and heat treatment. This study suggested that fabrication method

can have an impact on the degradation level because it can influence the chemistry by leading to different levels of imidization in the polymer.

It is clear that the need for a more accurate kinetic reaction model still remains. The degradation behavior at use temperatures (150-250°C) needs to be well understood. The quantification of oxidative reactions is more important than that of thermal reactions as material is exposed to air when in use, and also because their effects outweigh those due to purely thermal reactions.

CHAPTER 3

PROBLEM STATEMENT AND APPROACH

3.1   PROBLEM STATEMENT

The focus of this research is to develop a model of the chemical degradation of a polymer matrix composite such that, given the external chemical environment and temperatures throughout the laminate, laminate geometry, and ply and/or constituent material properties, and the concentration of diffusing substances throughout, we can calculate the metrics of chemical degradation, as functions of time and position throughout the laminate.

3.2   APPROACH

The approach consists of both analytical and experimental work. The analysis provides insight into the physical mechanisms and can be used for building models. These models are also useful for interpreting and reducing test data. The ultimate goal of the analysis is to provide a capability for predicting composite degradation behavior. Experiments improve the understanding of the chemical degradation in service conditions, and allow the building of an advanced model that eliminates the shortcomings of the previous models. Long term isothermal tests were conducted at various temperatures. The experimental data was utilized for obtaining the coefficients of the advanced analytical model and provided verification of the analytical approach. The data, along with the previous work, also provided

useful insights for future testing.

3.3   ANALYTICAL TASKS

The analysis comprises a basic chemical reaction model. An Arrhenius reaction model is used for describing the thermal and oxidative reactions. Mass loss (or gain) is used as a degradation metric. The entire mass is divided into smaller mass fractions, some of which do not react. Each of the reacting mass fractions is assumed to be attacked by one chemical reaction which alters the amount of mass remaining after thermal exposure. Three different reactions are considered. Two lead to mass loss, and one leads to mass gain. A negative mass fraction is used to model the mass gain behavior observed during experiments. The analysis includes the temperature range for which experiments were conducted (150 to 300°C).

The analysis is implemented through the use of an explicit time-step finite difference computer code. Inputs to the analysis are the exposure temperature as a function of time. Degradation states within the material are calculated as functions of exposure time. The analysis was used to reduce mass change data from aging experiments on powdered specimens to a set of chemical reaction constants. Finally, model predictions incorporating chemical reactions were correlated with the mass loss data obtained in aging tests conducted during the course of this research, and also some of the experimental results from tests on neat resin powder carried out by Cunningham [1].

3.4   EXPERIMENTAL TASKS

All materials used in the course of this research were manufactured at the NASA Lewis Research Center. Neat PMR-15 resin samples are

considered. Isothermal tests on powdered resin specimens are carried out in both inert and oxidative environments. The use of powders allows the decoupling of purely chemical effects from diffusion controlled effects. The inert atmosphere is used so as to provide data for the purely thermal effects. A new low cost test method is developed, and tests are carried out for a large variety of conditions, for up to 200 hours. The results, and the correlation with the analysis, provide insight into accurate methods for determining aging behavior in this class of materials.

CHAPTER 4

ANALYTICAL METHODS

The basic analytical approach is described in this chapter. The chemical reaction model used for quantifying the degradation is explained here. The model uses Arrhenius type of reactions to describe the mass changes in the material. The procedure for reducing test data to obtain the reaction coefficients, and the method for implementing the model, are detailed.

4.1 DEGRADATION MODEL

Chemical reactions are used to model the degradation behavior. The analytical treatment given here is similar to that used by Cunningham [1] and McManus and Chamis [29]. The reactions are considered to take place inside an infinitesimal control volume containing a mass m_o of matrix material. The fibers are assumed to be stable. The matrix material is assumed to consist of different components that are available for various reactions. A mass m_i is defined as the mass that would be lost (or gained) due to the completion of a set of reactions involving component i. A mass fraction y_i is defined as the ratio between the mass of component i and the overall mass

$$y_i = \frac{m_i}{m_o} \qquad (4.1)$$

A negative mass fraction is used to indicate the amount of mass added due to

a weight gain reaction. A conversion metric α_i is used to quantify the degradation of mass fraction y_i. When α_i is equal to zero, no degradation has taken place; when α_i is equal to one, the mass fraction is entirely lost (or gained). The rate at which mass changes from the control volume due to degradation of component i is

$$\frac{\partial m_i}{\partial t} = -m_o y_i \frac{\partial \alpha_i}{\partial t} \tag{4.2}$$

Note that summation notation is *not* used here. The total mass change for component i, over a time period t is given by

$$\Delta m_i = \int_0^t \frac{\partial m_i}{\partial t} dt \tag{4.3}$$

Finally, the mass change for the control volume is

$$\Delta m = \sum_{\text{all } i} \Delta m_i \tag{4.4}$$

All of the above considers the mass loss at a point within the material, which is not a measurable quantity. In a finite specimen of volume V, we measure the total mass change and mass change rate

$$\Delta M = \int_V \Delta m dV \tag{4.5}$$

$$\frac{\partial(\Delta M)}{\partial t} = \int_V \frac{\partial(\Delta m)}{\partial t} dV \tag{4.6}$$

Finally, in some cases certain mass fractions will not react. A final mass m_f is defined as the sum of the unreacting mass fractions

$$m_f = m_o \sum_{i \subset unreacting} y_i \tag{4.7}$$

A normalized mass change, which reaches a value of one when all reactions have completed, is then defined as

$$\Delta m' = \frac{\Delta m}{m_o - m_f} \tag{4.8}$$

The conversion metric, α_i, is defined here in terms of the normalized mass change for each component i at any time t

$$\alpha_i = \Delta m_i' = \frac{\Delta m_i}{m_{o_i} - m_{f_i}} \qquad (4.9)$$

where m_{o_i} and m_{f_i} represent the initial and final masses of component i respectively. For weight adding reactions $m_{o_i} = 0$, and for weight losing reactions $m_{f_i} = 0$.

Arrhenius reaction kinetics are assumed for the chemical reactions acting on the different mass fractions. Reaction rates for each material component i are related to the conversion metric, α_i, and to the absolute temperature, T, by different and independent functions. A complete kinetic description of a chemical reaction requires the characterization of both, the rate (temperature-dependence) function $F'(T)$, and the conversion-dependence function $F(\alpha_i)$ [6]. Generally, reaction rates increase with temperature. At high values of α_i the reaction rate will typically slow down due to the decreasing amount of material available to the reaction.

The rate constant $F'(T)$ is a function of temperature only, whereas $F(\alpha_i)$ is some function of conversion, α_i. Typically, $F'(T)$ is assumed to follow an Arrhenius-type expression, and so

$$F'(T) = k_i \exp\left(\frac{-E_i}{RT}\right) \qquad (4.10)$$

where k_i is the reaction rate constant defining the frequency of occurrence of the particular reaction configuration, E_i is the activation energy which represents the energy barrier that must be surmounted during transformation of reactants into products, and R is the real gas constant. $F(\alpha_i)$ is commonly expressed as $(1 - \alpha_i)^{n_i}$ assuming nth-order kinetics, giving

$$\frac{\partial \alpha_i}{\partial t} = k_i(1-\alpha_i)^{n_i} \exp\left(\frac{-E_i}{RT}\right) \qquad (4.11)$$

In cases where the reactions are controlled by the concentration of a diffusing substance, a modified form of Eq. 4.11 is used

$$\frac{\partial \alpha_i}{\partial t} = k_i(1-\alpha_i)^{n_i} c_s^{m_{si}} \exp\left(\frac{-E_i}{RT}\right) \qquad (4.12)$$

where c_s is the concentration of the diffusing species and m_{si} defines the order of the concentration dependency.

All of the expressions derived thus far assume that only a single reaction acts on each of the mass fractions. For the general case where multiple reactions can occur, each mass fraction y_i can be attacked by a number of reactions j. The reactions rates in, say, an oxidative atmosphere can then be fully described by

$$\frac{\partial \alpha_{ij}}{\partial t} = k_{ij}(1-\alpha_i)^{n_{ij}} c_s^{m_{ij}} \exp\left(\frac{-E_{ij}}{RT}\right) \qquad (4.13)$$

where c_s is the concentration of the diffusing oxygen. Again, summation is *not* implied here. The reaction rate constant k_{ij}, activation energy E_{ij}, and reaction order n_{ij} are needed to fully characterize each reaction. The oxygen concentration dependence m_{ij} is zero for thermal (non-oxidative) reactions, and must be specified for oxidative reactions. The reduction of mass fraction of component i is calculated from

$$\frac{\partial \alpha_i}{\partial t} = \sum_{\text{all } j} \frac{\partial \alpha_{ij}}{\partial t} \qquad (4.14)$$

$$\alpha_i = \int_0^t \frac{\partial \alpha_i}{\partial t} dt \qquad (4.15)$$

Note that none of the quantities in here are tensors. The notation employed in these equations was chosen as a convenient method in which to express the occurrence of multiple, simultaneous reactions. This is the

28

general form of the chemical degradation model. The specific model used in this research considered that only one chemical reaction acted on each component. The additional complexity of multiple reactions acting on each component was not required to model the observed chemical reactions.

4.2 DETERMINATION OF KINETIC CONSTANTS

No standard method is available in the literature for determining kinetic constants from mass loss data for isothermal tests. Reaction constants for the model were obtained by reducing the data using curve-fitting techniques.

The mass loss/gain data collected from isothermal tests in air suggests that a minimum of three reactions are required to describe the chemical degradation. Determining the mass fraction on which each reaction acts, and the three kinetic constants that specify each reaction, is necessary for completely describing the model. Each reaction is described using three constants: activation energy E_i, order of reaction n_i, and rate constant K_i, where

$$K_i = k_i c_s^{m_{si}}$$
(4.16)

and $c_s^{m_{si}}$ is constant because the oxygen concentration does not change as a function of time or position.

Observed experimental data, detailed in Chapter 6, indicated the presence of two reactions acting on relatively small mass fractions and a reaction acting on a large mass fraction. Once of the small mass fraction reactions led to mass gain. The mass gain reaction was modeled using a Arrhenius type of reaction acting on a negative mass fraction. None of the previous models include mass gain behavior. The small mass fraction

reactions with mass loss (reaction 1) and mass gain (reaction 2) showed saturation behavior (no more mass loss or gain is seen). The mass fractions for these reactions were determined using the normalized mass loss/gain seen at saturation stage. The large mass fraction for the third reaction was estimated using a numerical search. After the mass fractions were obtained the kinetic constants were determined using a curve-fitting procedure in two steps. The details of this curve fitting procedure are described in section 4.4.

4.3 MODEL IMPLEMENTATION

The model was implemented for an infinitesimal volume subjected to isothermal heating in air. Three reactions were considered, all of which were assumed to be oxidative. As the tests were conducted on powdered material in air, no variation in the oxygen concentration was considered. Initial conditions consisted of $\alpha_i = 0$ for all three reactions. The reaction rate constant K_i as described in Eq. 4.16 was used. E_i, n_i, and K_i were specified for each reaction along with time t. The rate of reaction was calculated using Eq. 4.12 and then multiplied by the corresponding mass fraction (Eq. 4.2) to get the rate of change of mass for each reaction. The rate of mass change for each reaction was then integrated over time t (Eq. 4.3) and then summed to obtain the total mass change (Eq. 4.4). Reactions that showed saturation reached state $\alpha_i = 1$ and then the reaction state did not change. All the mass changes were calculated as normalized mass loss or gain. The model was implemented using an explicit time-step finite difference computer code

4.4 DATA REDUCTION IMPLEMENTATION

Observation from the experimental data showed the presence of a minimum of three different reactions. There is a possibility of more than 3

30

reactions being active in this temperature range (150-300°C), however it was thought that three reactions would be sufficient to model the degradation behavior observed in these isothermal aging tests.

The coefficients for the three reactions in the model and the mass fractions on which they act were obtained from the experimental observations. We assumed a small mass loss reaction (see 150°C), a small mass gain reaction (see 175-200°C), and a mass loss reaction that affected a large mass fraction. The saturation behavior seen in 150-200°C test was utilized for obtaining the mass fractions for the two small mass change reactions. The large mass fraction for the third reaction was estimated using a numerical search. No distinction was made between thermal and oxidative reactions. All reactions were modeled as being of the form

$$\frac{\partial \alpha_i}{\partial t} = K_i (1 - \alpha_i)^{n_i} \exp\left(\frac{-E_i}{RT}\right) \tag{4.17}$$

where K_i is defined in Eq. 4.16 for an oxidative reaction. In case of a thermal reaction, $K_i = k_i$ was assumed. The three coefficients for each reaction consisting of rate constant K_i, reaction order n_i, and activation energy E_i were estimated using an optimization procedure in two steps. In the intermediate step, each reaction was modeled using C_i and n_i, where

$$C_i = K_i \exp\left(\frac{-E_i}{RT}\right) \tag{4.18}$$

Each reaction was described as

$$\frac{\partial \alpha_i}{\partial t} = C_i (1 - \alpha_i)^{n_i} \tag{4.19}$$

The degradation state for each reaction was determined using the explicit time-step finite difference formulation

$$\alpha_i(t + \Delta t) = \alpha_i(t) + \frac{\partial \alpha_i}{\partial t}(t) \times \Delta t \tag{4.20}$$

31

where $\alpha_i = 0$ at $t = 0$. The reaction state calculated in this manner was multiplied by the respective mass fraction for all the reactions to obtain the total normalized mass loss/gain. These results were compared with the data obtained from experiments and the least squares error was calculated. Values for C_i and n_i were obtained by minimizing the least squares error for each temperature. This was carried out for data at all the seven test temperatures (150-300°C in steps of 25°C). The n_i values were found to be in a narrow range for each reactions, as expected. The reaction order in the Arrhenius type of reaction does not change with temperature. The values obtained for C_i varied a lot because of the strong dependence on temperature. The MATLAB code utilized for this purpose is given in Appendix A along with all the other codes used during the course of this research.

In the next step, each reaction was quantified using all the three coefficients K_i, n_i and E_i. The reaction states for each reaction were calculated using the finite difference formulation from the previous step. The normalized mass loss (or gain) was obtained as in the previous step. Estimates of mass change were obtained for all the seven temperatures and then compared to the experimental data. The least squares error obtained from comparison with each data set was normalized by the mean mass change for that temperature. The sum of such normalized least squares error for all the data sets was used as the error function. This error function was minimized using a standard optimization tool available in MATLAB (version 5.2). Constraints were placed on the values of reaction order as per the ranges obtained in the previous step. This constrained optimization is solved using the Levenberg-Marquardt method by the optimization tool. The coefficients so obtained were used for further comparisons of the model with data from previous researchers.

CHAPTER 5

EXPERIMENTAL PROCEDURES

Experiments were carried out to obtain data for the chemical degradation model described in Chapter 4. The data obtained from experiments gave valuable insights into the physics of the problem in addition to helping obtain the reaction and mass fraction coefficients. The new cost-effective experimental method is described along with details about specimen preparation, the set-up and data collection. Only neat PMR-15 resin samples were used.

Only neat resin specimens in powder form were used in this investigation. The test matrices were designed based on recommendations by Cunningham[1], and the fact that the in-use temperature range for this material is from 150 to 250°C. The material is also known to give off noxious fumes at a temperature of 350°C and beyond. Cunningham [1] had also recommended the use of specimens with large surface area to volume ratios in determining kinetic parameters. Reaction coefficients estimated from experiments conducted on finite-sized specimens may be confounded because of diffusion effects. Oxidative reactions were shown to be limited by the amount of oxygen available and hence powdered specimens were utilized for eliminating the diffusion effects. The test matrices were designed in such a way as to allow the necessary coefficients to be extracted from the data and also to provide sufficient data to allow a complete validation of the modeling approach.

The material systems used in this study was PMR-15 neat resin. All materials were manufactured at the NASA Lewis Research Center. The material was initially cured in plates and was then reduced to powder form. This ensured that the initial chemical state of the material was the same as that used in real structures. The test matrix used for the isothermal heating experiments is shown in Table 5.1. Isothermal heating experiments were carried out on PMR-15 neat resin powder in nitrogen and air. This was done with the aim of allowing the quantification of the kinetic parameters in both thermal and oxidative atmospheres without the additional complexity introduced by diffusion dominated effects.

5.1 MATERIAL MANUFACTURE AND PREPARATION

All specimens were manufactured at the NASA Lewis Research Center using standard manufacturing procedures developed for the PMR polyimides. The details of these procedures may be found in [34]. Two PMR-15 neat resin panels (both 102 mm x 102 mm and approximately 3 mm thick) were used during this study. After curing, all panels were subjected to a 16 hour free-standing post-cure in air at 316°C.

Narrow strips (approximately 5 mm wide) were cut from the neat resin panels using a clean, sharp knife edge. These strips were then broken into several small pieces and placed into a standard coffee grinder. To avoid the problem of plastic shards from the grinder blade casing contaminating the material (as previously encountered by Cunningham [1]), a grinder with metal casing was obtained. A custom steel lid was manufactured for use instead of the plastic cover. Specimens were subjected

Table 5.1   Neat Resin△ Isothermal Exposure Test Matrix

	Atmosphere	
Isothermal Exposure temperature	Air	Nitrogen
125°C	1	1
150°C	1	
175°C	1	
200°C	1	1
225°C	1	
250°C	1	
275°C	1	
300°C	1	1

△   All specimens in form of fine powders.

to grinding for about five minutes. The grinder was turned off after every two minutes for about thirty seconds to avoid over-heating the motor. The powder which was produced in this manner was then sifted through calibrated sieves to obtain the required grade of powder for analysis. A fine, light-brown powder was obtained from each sample through the use of this technique. Tests conducted by Cunningham [1] had indicated that the particles obtained through the use of a No. 40 USA Standard Testing Sieve (425 micron grating) were sufficiently small to ensure that the effects of diffusion on the weight loss behavior in oxidative environments would be negligible. All of the powder was sifted through a No. 40 sieve.

All powders produced in this manner were placed in small, unsealed glass jars into the oven for 2 hours at 125°C to remove any residual moisture. Due to the large surface area of the particles, the removal of moisture from the powder is achieved in small amounts of time. This large surface area also has a secondary effect which is to allow moisture to diffuse very quickly back into the powder. The neat resin powder was found to be very hygroscopic, rapidly absorbing moisture from the air upon removal from the oven. The glass jars were immediately sealed after removal from the oven and the powder was stored like this until testing.

5.2 EXPERIMENTAL PROCEDURE FOR ISOTHERMAL TESTS

5.2.1 Experimental Set-up

All powdered neat resin samples were aged in a thermal environment chamber. The chamber used electric resistance rods for heating and a maximum temperature of 427°C could be achieved. A stainless steel rack made using four rods and three rectangular plates with holes, was used to

support the specimens within the chamber. The powdered sample was placed in an aluminum pan (dia. 35 mm) in the same location close to the chamber bottom for each test. Internal chamber dimensions were 30.2 cm x 10.2 cm x 10.2 cm (12" x 4" x 4"), and the sample pan was placed at a height of 3" from the bottom.. A schematic of the set-up is shown in Figure 5.1. The specimens were shielded from direct heat radiation from the heating rods and were heated by fan-circulated air only. The temperature of the chamber was controlled through the use of an Omega temperature controller. This microprocessor-based controller could be programmed to any user-defined thermal profile consisting of a series of linear segments. A single J-type thermocouple provided feedback to the controller. The temperature gradient between the sample pan location and the controller thermocouple was minimized. Over 100 tuning runs had been carried out in a previous study to determine the optimum controller tuning settings and feedback thermocouple location [35]. These settings were not altered in the current study.

5.2.2 Tests in Air

A clean aluminum pan, spatula and pincers were used for each experiment. This apparatus was cleaned with water and than with methanol and then dried for 15 minutes in a clean-air hood. A new pan was used for each experiment. The steel rack and inside of the chamber were cleaned using a wet paper towel before each experiment. The chamber was then heated to 125°C and held there for 15 minutes before starting the experimental run.

Steel stand
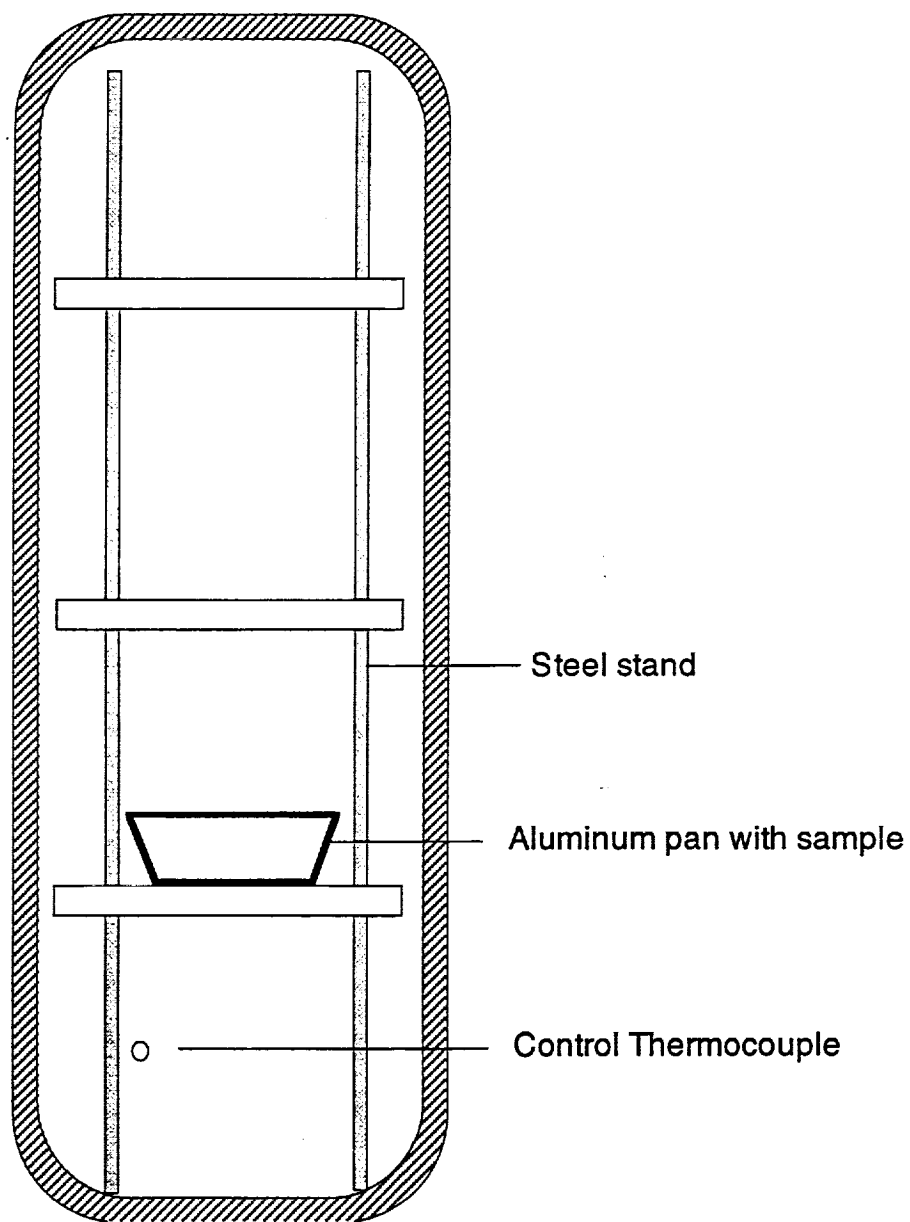
Aluminum pan with sample

Control Thermocouple

Figure 5.1   Schematic of specimen and thermocouple location in thermal environment chamber (not to scale).

AE 100 Mettler balance with a least count of 0.1 mg was used for weighing the pan and sample. The clean pan was weighed first, and then a sample of about 600 mg was placed in it. A spatula was used for removing the powder from the glass jars. The weighing balance was recalibrated and its leveling checked before each experiment. The sample pan was moved using pincers only, and the pincers were cleaned periodically and kept free of dust throughout the experiment. The pan was placed on the lowest shelf inside the chamber. The sample was then heated to 125°C and held for two hours. The pan was removed from the chamber and weighed at the end of these two hours. The sample mass obtained from this measurement was utilized during all further calculations. The temperature was then ramped up to the test temperature and then held there for a duration in excess of 200 hours.

The sample pan was removed periodically for weight measurements. The chamber door was opened, the pan was removed, and the door was immediately closed. The pan was then weighed using the sensitive balance and then put back into the thermocycling chamber. This procedure lasted less than a minute. The test chamber temperature dropped because the door was opened twice during each measurement. However, the test temperature was restored in less than five minutes due to the large thermal mass of the chamber. As tests were conducted in excess of 200 hours, and readings taken with an average gap of six hours (360 minutes) this temperature drop was not considered in further calculations and the sample was assumed to be at a steady temperature throughout the duration of the test.

A test was conducted in which a pan with powdered resin sample was held at 125°C for over 200 hours. No reactions are known to occur at this temperature and this experiment was conducted to study the extent of

possible scatter and any other sources of error. The weighing balance takes a few seconds to give a steady reading. This reading can be affected by any potential moisture absorption during this period. The readings showed a variation of +1.0 mg to -1.1 mg. Lack of any trend in this data showed that the sample was not being blown away by the circulation fan and that error due to sources such as moisture absorption was small (0.2%).

5.2.3 Tests in Nitrogen

Additional parts were used in the set-up for conducting isothermal tests in nitrogen. Nitrogen cylinders with 5 PPM impurities were used during these test. The cylinder was connected to a two-stage regulator. The maximum pressure of gas in the cylinder was 2000 psi. The second stage had a delivery pressure from 0 to 150 psi. The gas was then fed to a flowmeter, which was then connected to a tube. The gas passed through a moisture/oxygen trap before reaching the solenoid valve on the thermocycling chamber. The trap had a specification of 0.5 PPM impurities. A schematic of the setup used for tests in nitrogen is shown in Figure 5.2. The gas pressure was maintained 40-50 psi above the atmospheric pressure and the gas flow was increased (from 596 ml/min. to 913 ml/min.) during the time of sample removal for weight measurement. The gas was maintained at a pressure to avoid any air leaking into the chamber during the experiment. The effect of air exposure during the weight measurements was assumed to be insignificant. This assumption was found to be incorrect after data from three different runs was reduced. The details of this error are discussed in Chapter 6 (Results).
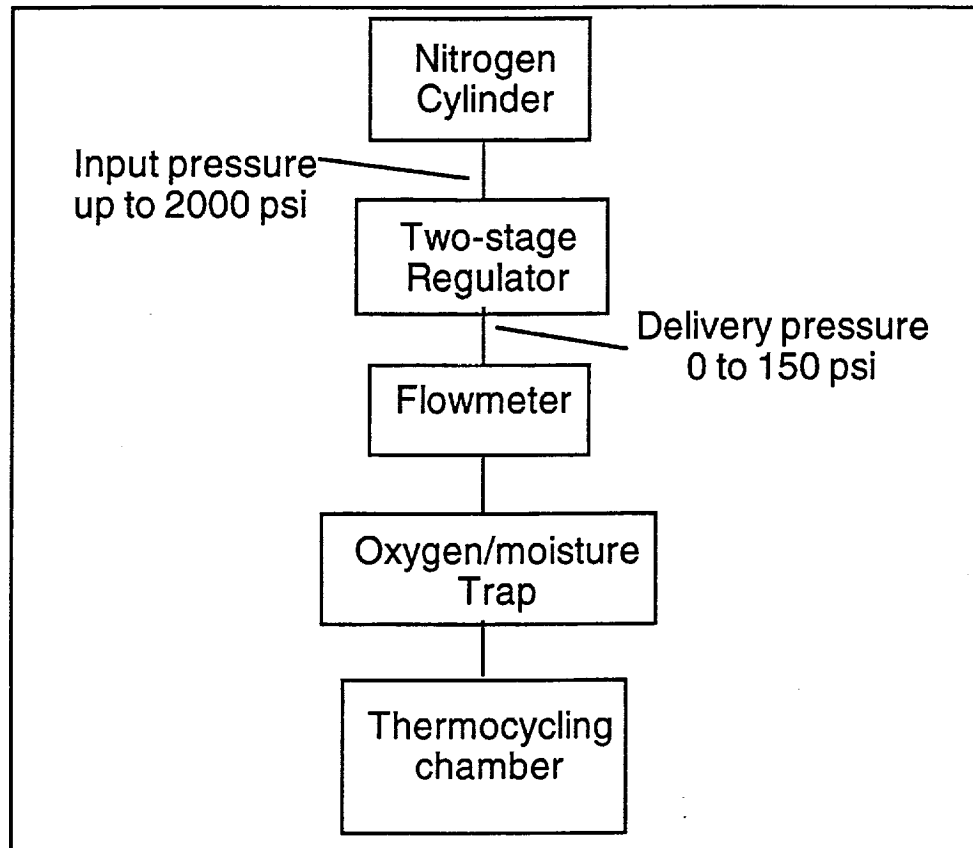
Figure 5.2   Schematic of atmosphere control system for aging tests in inert
atmosphere

CHAPTER 6

RESULTS AND DISCUSSION

In this chapter the experimental data and the analytical results obtained from the model are presented. Long term isothermal tests were conducted in oxidative environment (air) and also in purely thermal environment (nitrogen). The data from tests in air was reduced to obtain the kinetic reaction coefficients, which served as input to the analytical model. The model was correlated with this data. A combined model, using this model with parts of the previous model of Cunningham [1] was used for correlating with some of the previous TGA data.

6.1 LONG TERM ISOTHERMAL AGING TESTS IN AIR

Isothermal aging tests in the oxidative environment were conducted for temperatures of 125 to 300°C in steps of 25°C. This temperature range was selected because the service conditions for this material range from 150-250°C. The results obtained are presented in the form of normalized mass loss plotted against time in hours. This data was then reduced using the procedure described in Chapter 4. A comparison of model predictions using these coefficients with the isothermal aging data is also presented.

6.1.1 Experimental Data

All tests were conducted on powdered specimens in order to separate the diffusion effects from the reaction chemistry. Each sample was heated at

125°C for two hours before it was heated to the test temperature and held there for a duration in excess of 200 hours. The sample mass measured at the end of two hours of heating was used as the original mass. The normalized mass loss $\Delta m_n(t)$ at time t was calculated using

$$\Delta m_n(t) = \frac{M_0 - M(t)}{M_0} \tag{6.1}$$

where M_0 is the original sample mass, $M(t)$ is the sample mass measured at time t.

A long term isothermal aging test was carried out at 125°C to estimate the experimental error. No reactions are known to occur at this temperature and this test was conducted to study the extent of possible scatter and any other sources of error. The sample was removed from the thermocycling oven for mass measurement periodically. The sample was exposed to the atmosphere during this measurement. The actual process of taking a measurement took a few seconds, mostly to allow the weighing balance to give a steady reading. The reading can be affected by any potential moisture absorption during this period. For a sample mass of about 600 mg the readings showed a variation of +1.0 mg to -1.1 mg. The normalized mass loss results obtained from this test are given in Figure 6.1. Lack of any trend in this data showed that the sample was not being blown away by the circulation fan and that error due to sources such as moisture absorption was small (0.2%).

Experimental results obtained from tests at different temperatures are shown in Figures 6.2 to 6.8. The test conducted at 150°C clearly shows the presence of a small mass fraction reaction, see Figure 6.2. After a duration of about 100 hours saturation behavior was seen (no further mass loss/gain). The maximum normalized mass loss value was 7.2 x10^{-3}. The mass fraction

Figure 6.1   Isothermal aging test in air at 125°C

Figure 6.2   Isothermal aging test in air at 150°C

Figure 6.3   Isothermal aging test in air at 175°C

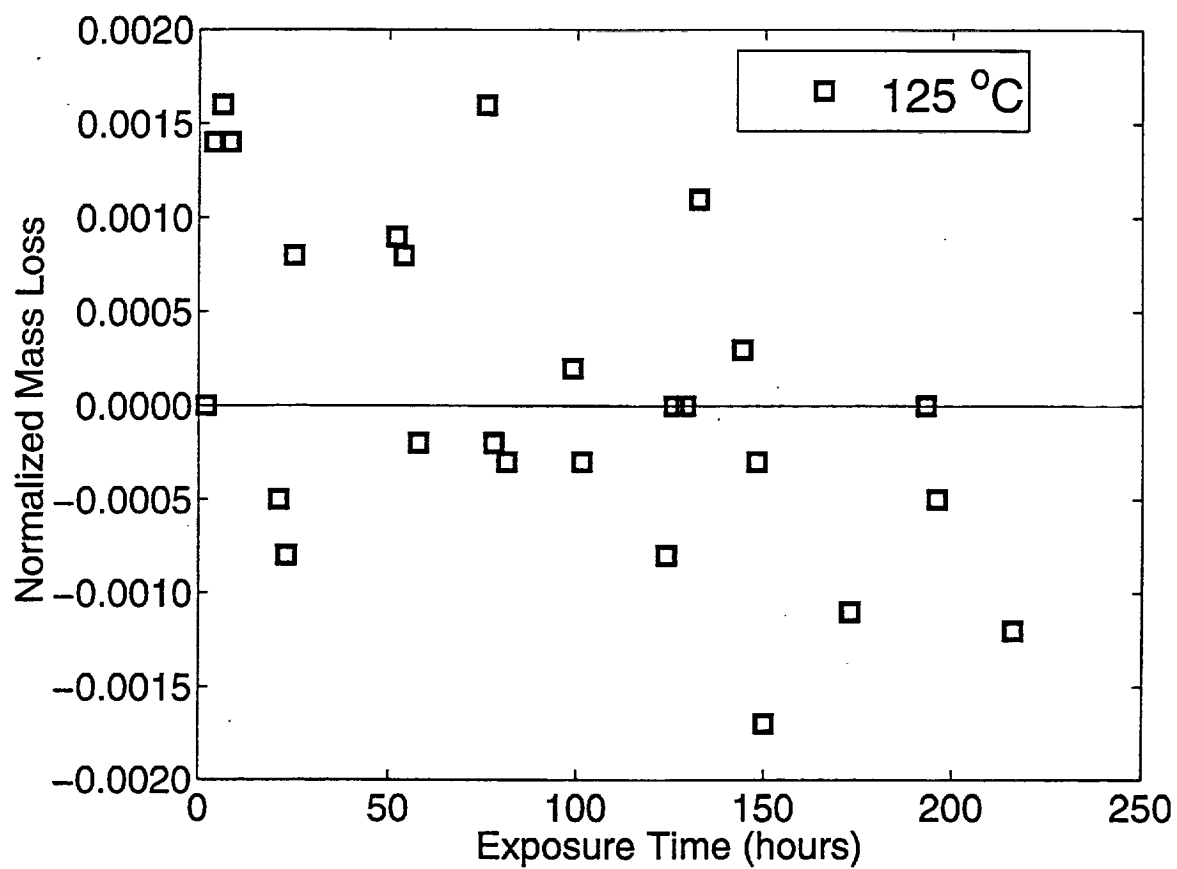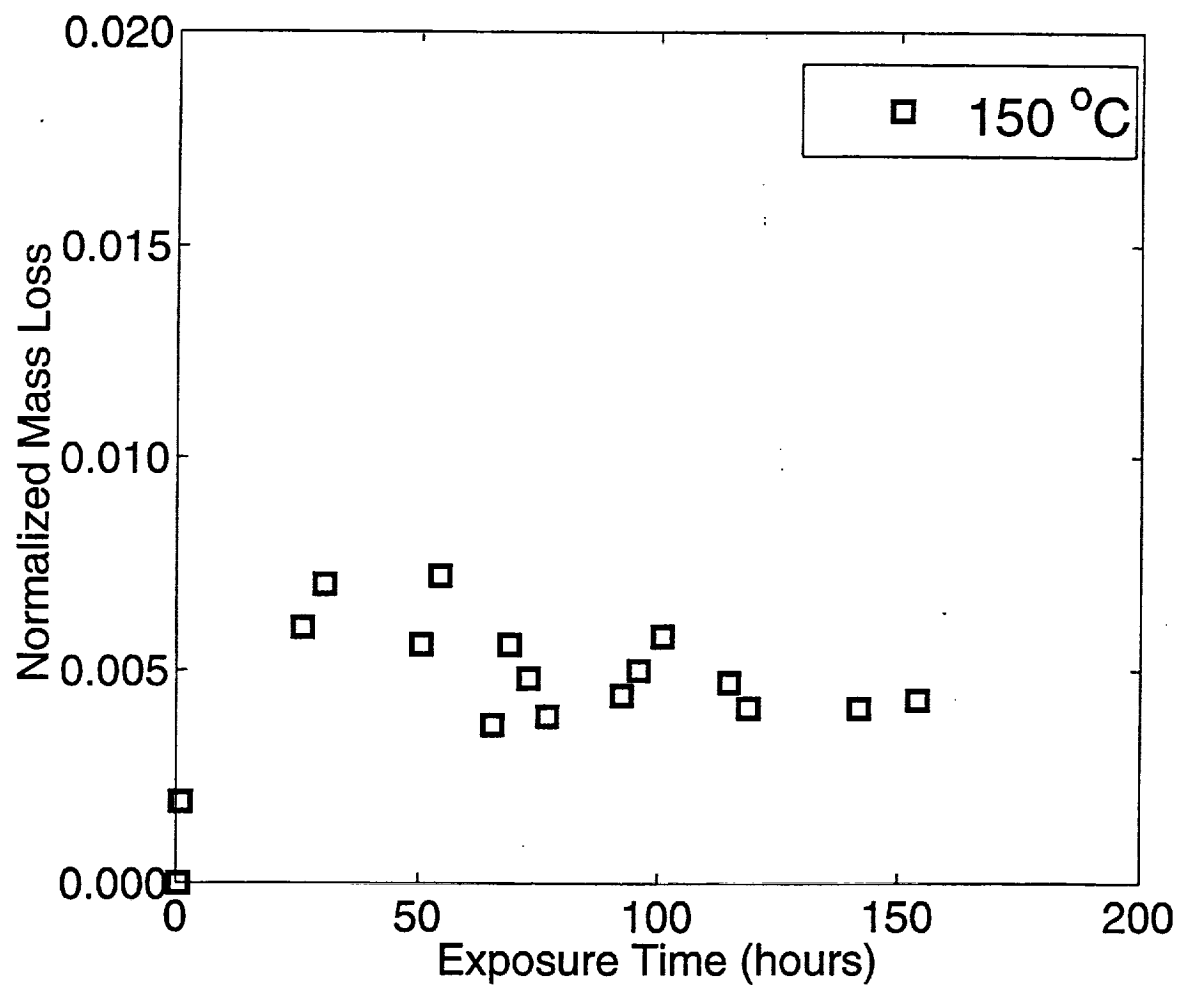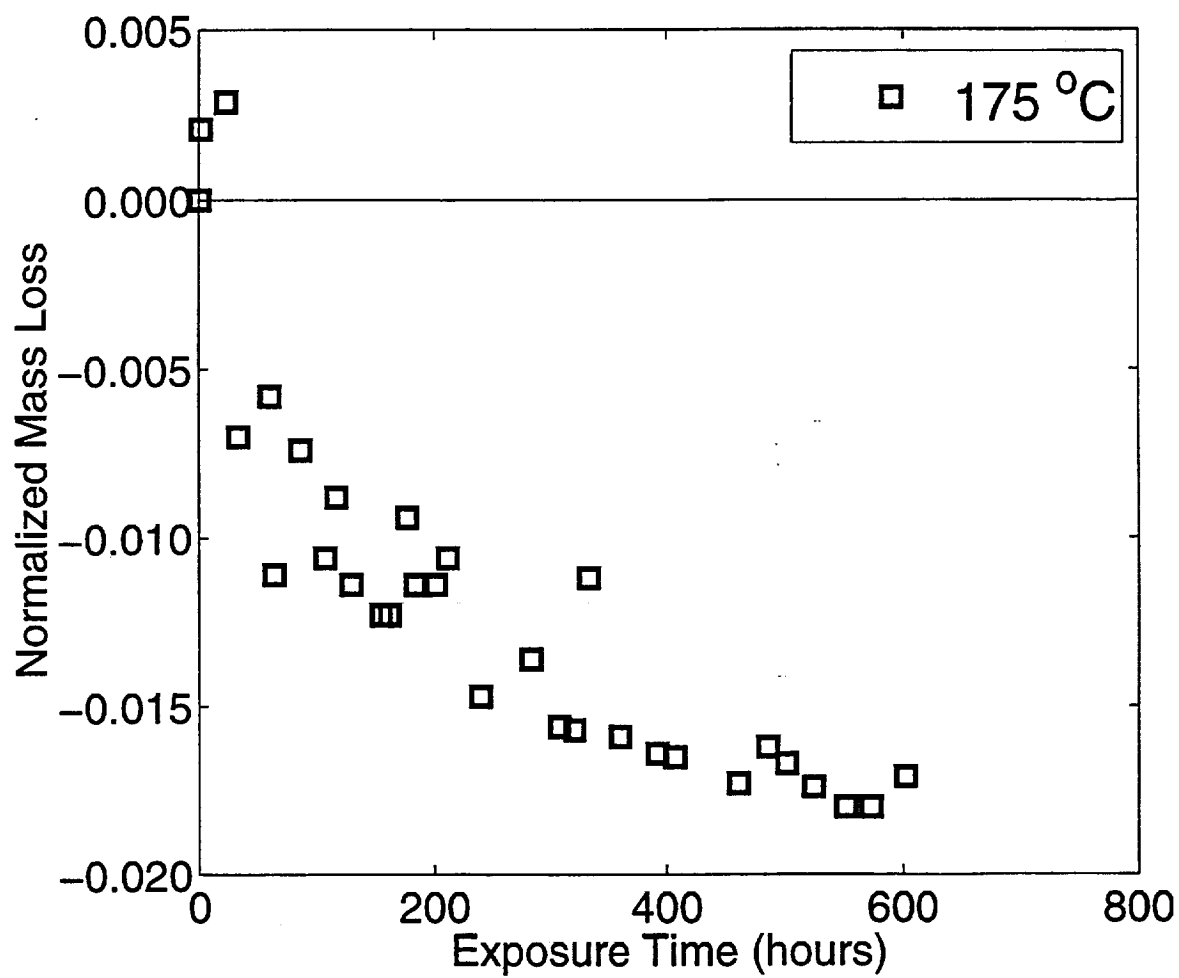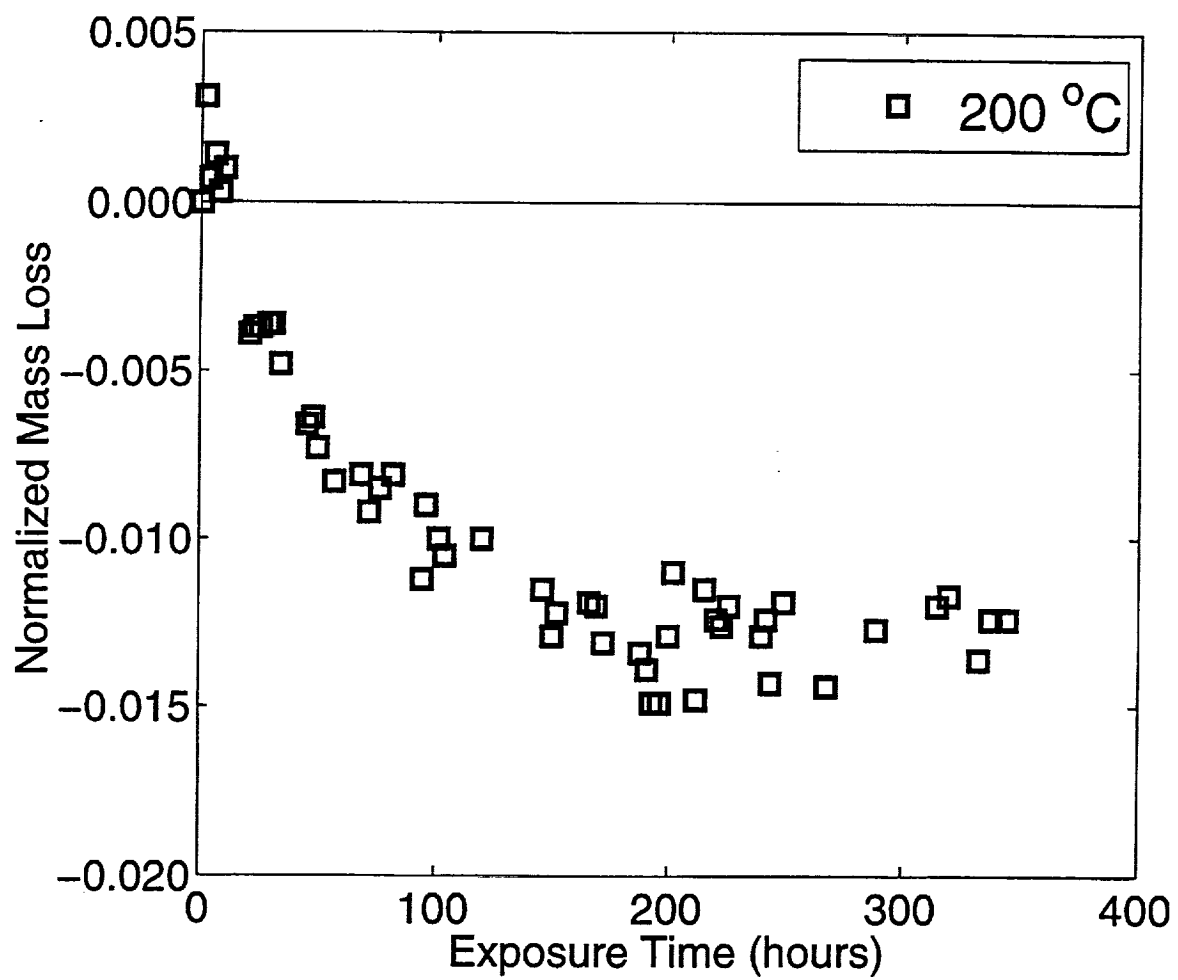Figure 6.4   Isothermal aging test in air at 200°C
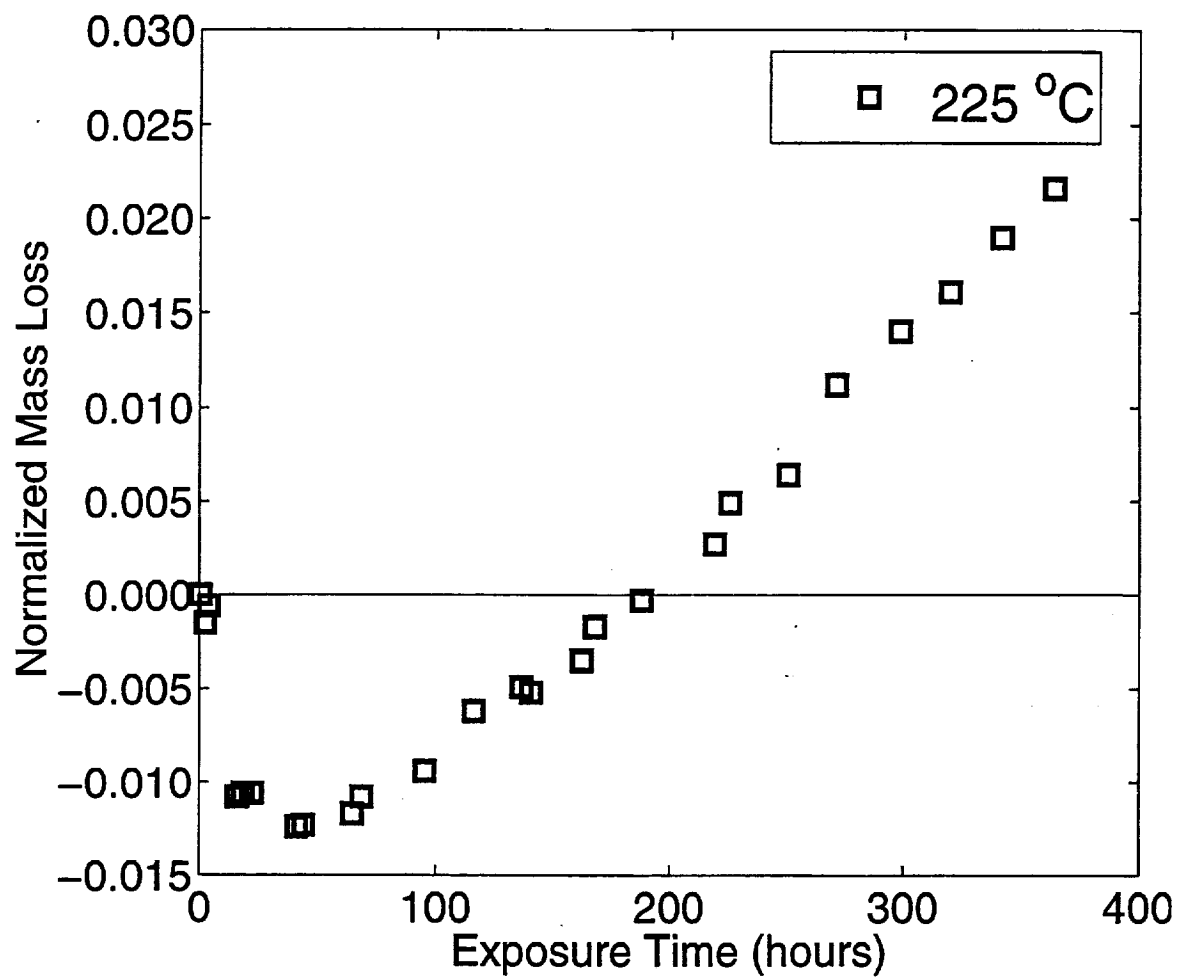
Figure 6.5   Isothermal aging test in air at 225°C
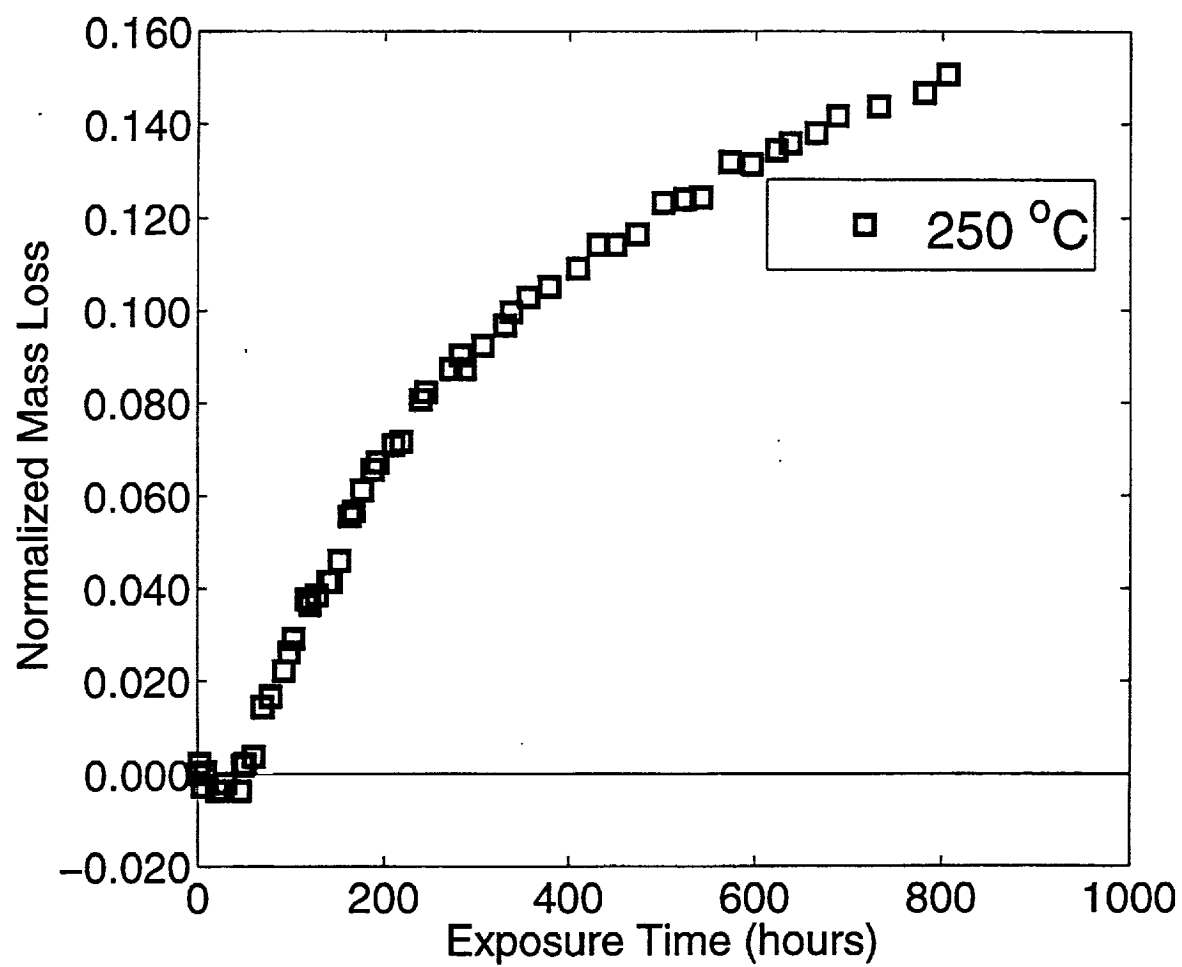
Figure 6.6   Isothermal aging test in air at 250°C
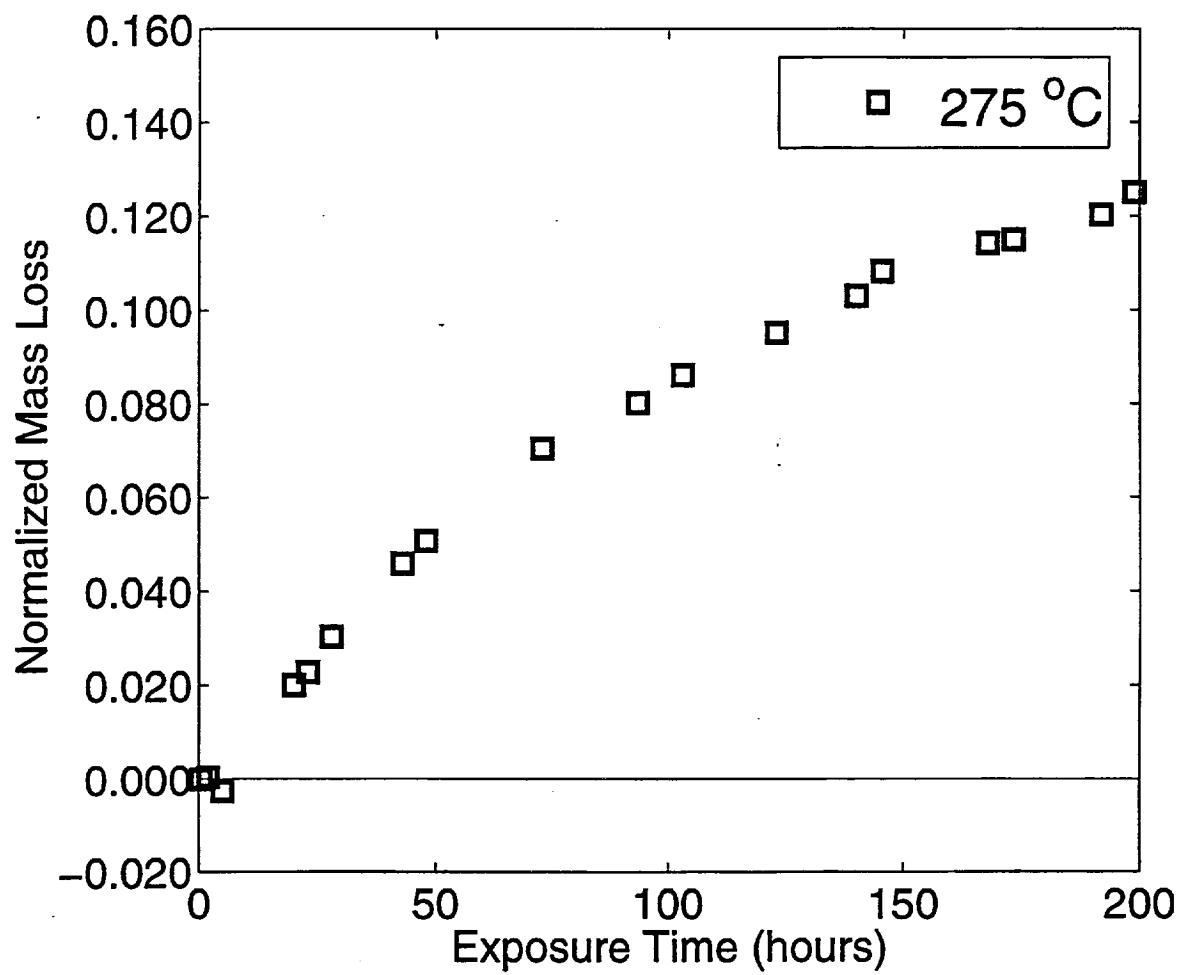
Figure 6.7   Isothermal aging test in air at 275°C
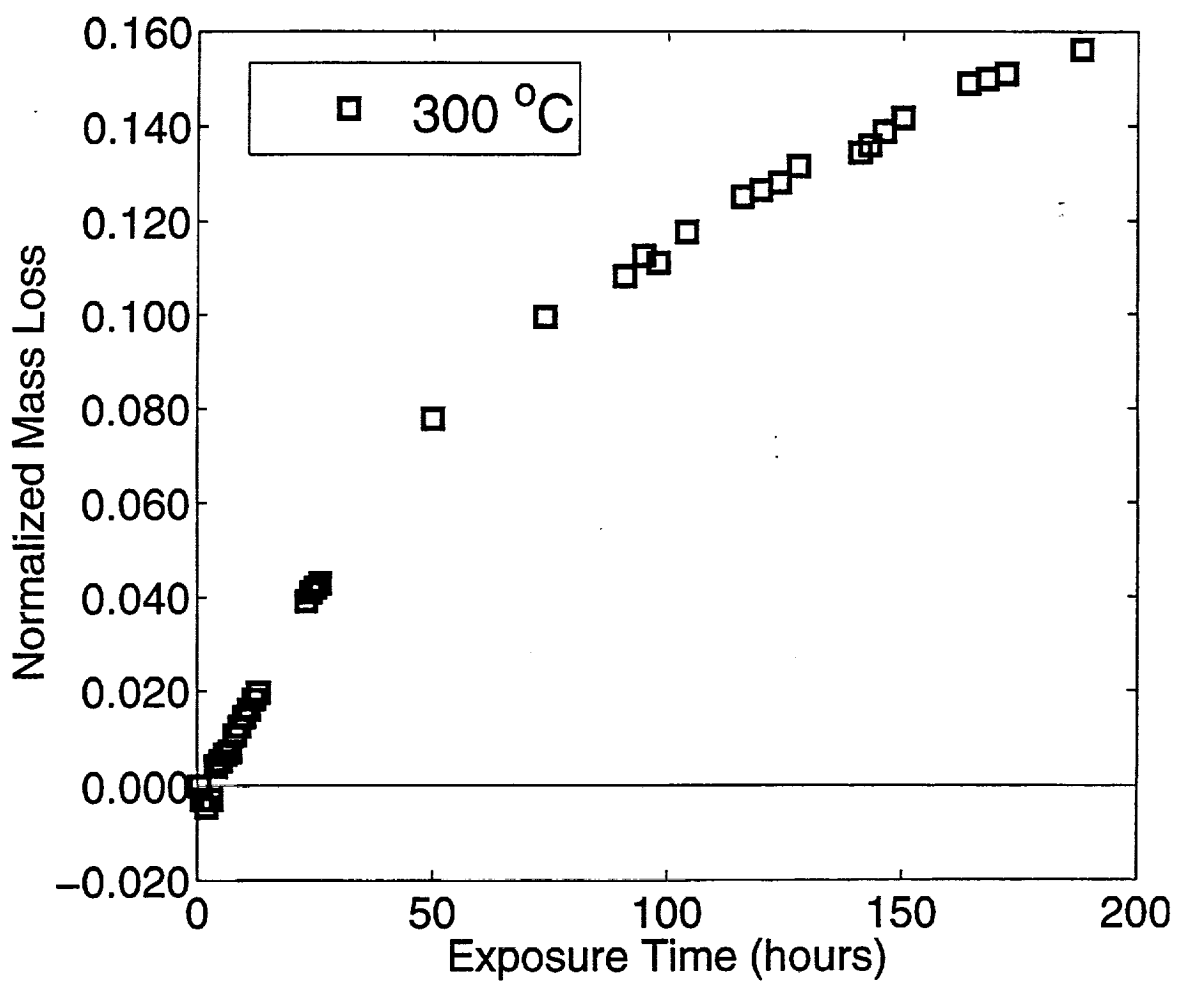
Figure 6.8   Isothermal aging test in air at 300°C

for this reaction was estimated using this saturation mass loss value. The data from the aging test at 175°C is given in Figure 6.3. These results show the presence of a small mass fraction weight gain reaction. Mass gain is shown as negative mass loss in this plot. Saturation in the mass gain behavior was observed after a duration of about 120 hours. The maximum normalized mass gain seen has a value of 18×10^{-3}. The mass fraction for the weight gain reaction was estimated using this value. The results from the aging test at 200°C, given in Figure 6.4, are very similar to that of the test at 175°C. However, the maximum mass gain value seen is lower at 14.9×10^{-3}, suggesting the presence of an additional reaction that leads to mass loss. The presence of an additional mass loss reaction is confirmed from the 225°C test results given in Figure 6.5. A clear transition from the domination of the mass gain reaction to the domination of mass loss reaction(s) is seen. Tests at higher temperatures show increasing levels of mass loss. No saturation behavior is seen in this case even after an aging period of over 1400 hours at 250°C, as seen in Figure 6.6. The tests at 275°C (Figure 6.7) and 300°C (Figure 6.8) show higher levels of mass loss and a trend similar to that seen at 250°C.

6.1.2 Data Reduction and Correlation

On the basis of experimental observations described in the previous sub-section, it was decided to use a three reaction model. This model consists of two small mass fraction reactions (reaction 1 - weight loss, reaction 2 - mass gain) and a large mass fraction reaction (reaction 3 - weight loss).

The mass fractions for reaction 1 was estimated using the highest normalized mass loss. value (7.2×10^{-3}) seen in the test at 150°C. Based on a

trial and error fit, considering the fact that weight addition reaction was slightly active, a mass fraction of 8 $\times 10^{-3}$ was selected for reaction 1.

The highest normalized mass gain value seen was 18 $\times 10^{-3}$. This mass gain was achieved after the saturation of first mass loss reaction, hence a mass fraction of 26 $\times 10^{-3}$ was assumed for reaction 2.

The tests at higher temperatures did not show any peaks or saturation. A numerical search for the mass fraction of reaction 3 in the range of 0.20 to 0.45 was carried out and the value (0.30) that gave the least root square error was used as the mass fraction for reaction 3.

Once the mass fractions were fixed, the kinetic constants were found as per the procedure described in Section 4.4. The kinetic constants for the three reactions are given in Table 6.1. These constants were presented in [36]. The mass fraction for reaction 3 shown here is slightly different than that presented in reference [36]. The current value gives somewhat better correlation with the data. The effect is not large. Note that the original form of reference [36] also contains an unfortunate error - the activation energies are incorrect by a factor of 10! The constants presented here, and also in reference [37], are correct.

The model was then implemented using these coefficients and compared with the experimental data, as shown in Figures 6.9 to 6.15. The model captures the mass loss (or gain) behavior quite well. Mass loss reaction domination at 150°C, followed by the mass gain reaction domination at temperatures 175°C and 200°C, and then the transition to mass loss reaction domination again, is captured. The model however, does not correlate well with the data obtained in the test at 300°C. It is thought that

Table 6.1   Coefficients for the new three reaction model

	Mass fraction y_i	Rate constant K_i	Activation energy E_i in KJ/mol	Reaction order n_i
1	0.008	12.8×10^8	109	1.0
2	-0.026△	8.67×10^8	124	2.1
3	0.300	9.65×10^8	155	3.6

△   negative mass fraction represents a mass gain reaction

Figure 6.9   Model comparison with isothermal aging test data in air at 150°C
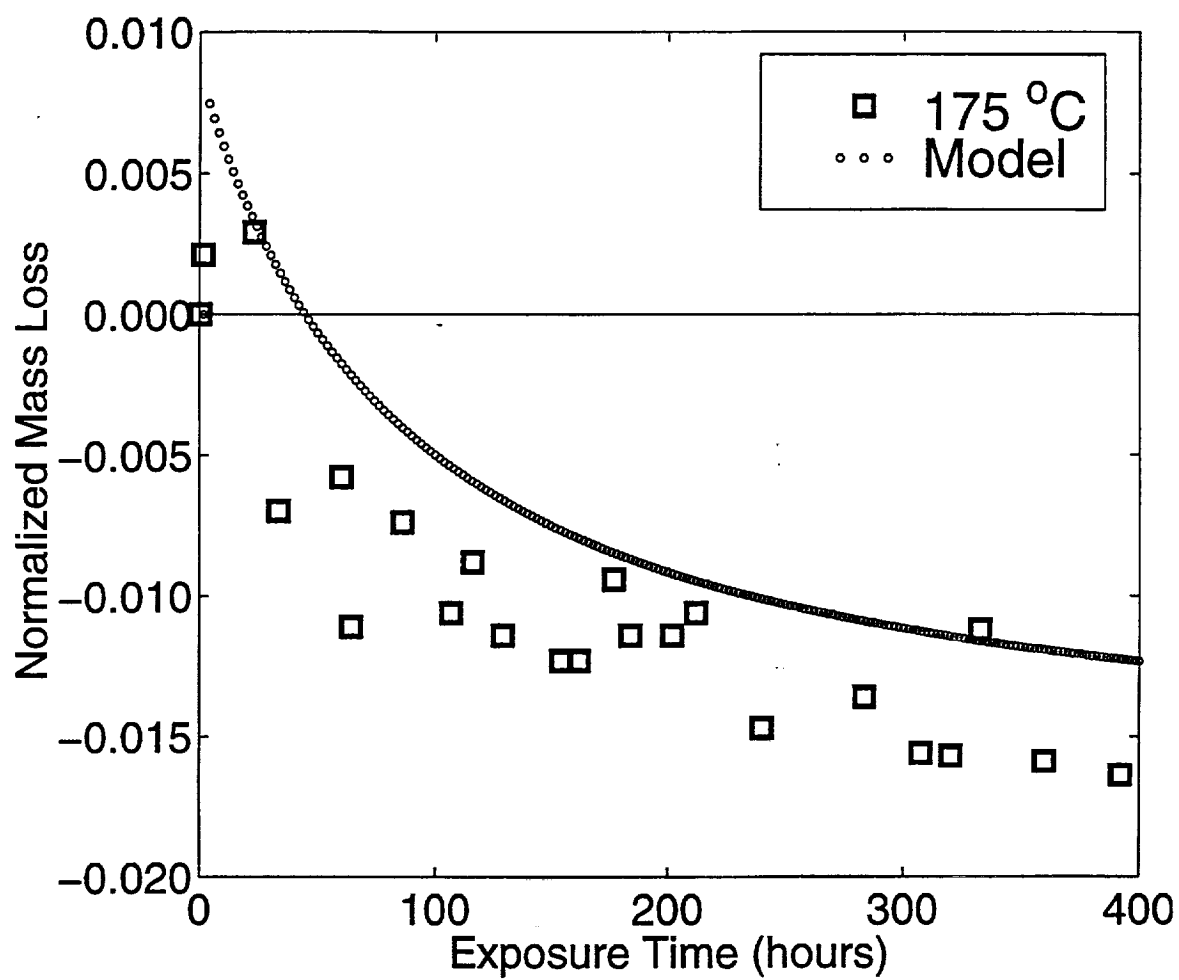
Figure 6.10   Model comparison with isothermal aging test data in air at 175°C
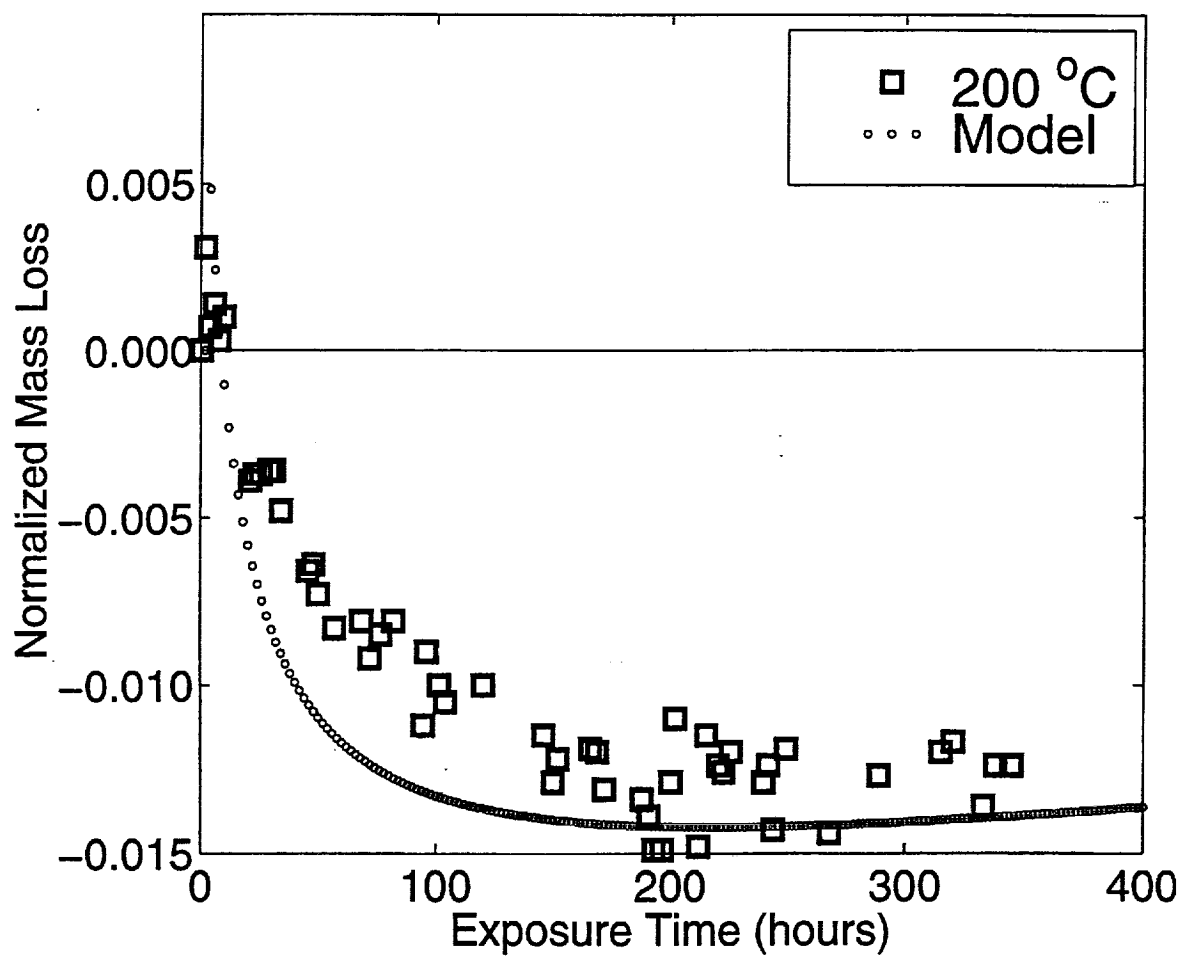
Figure 6.11   Model comparison with isothermal aging test data in air at
200°C
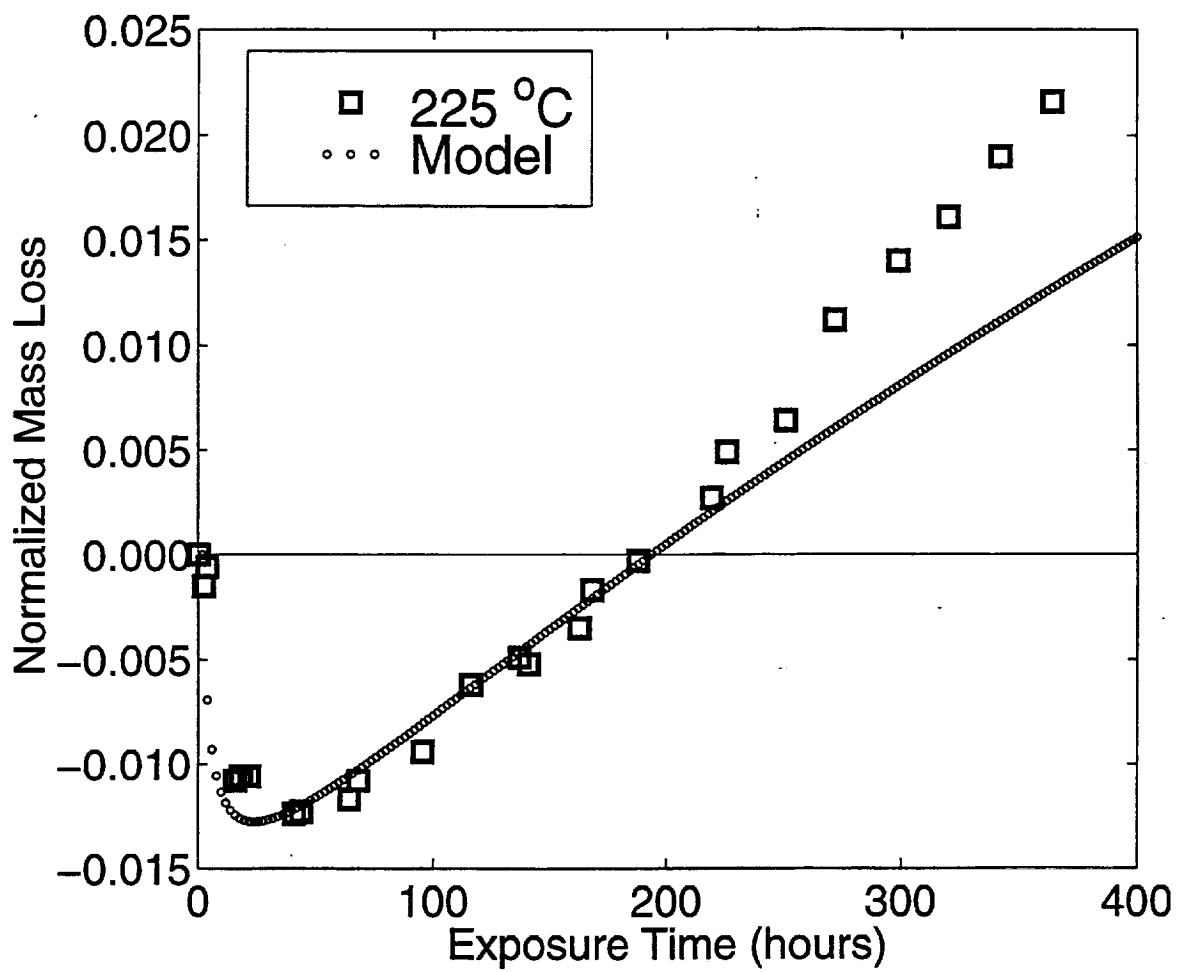
Figure 6.12   Model comparison with isothermal aging test data in air at
225°C
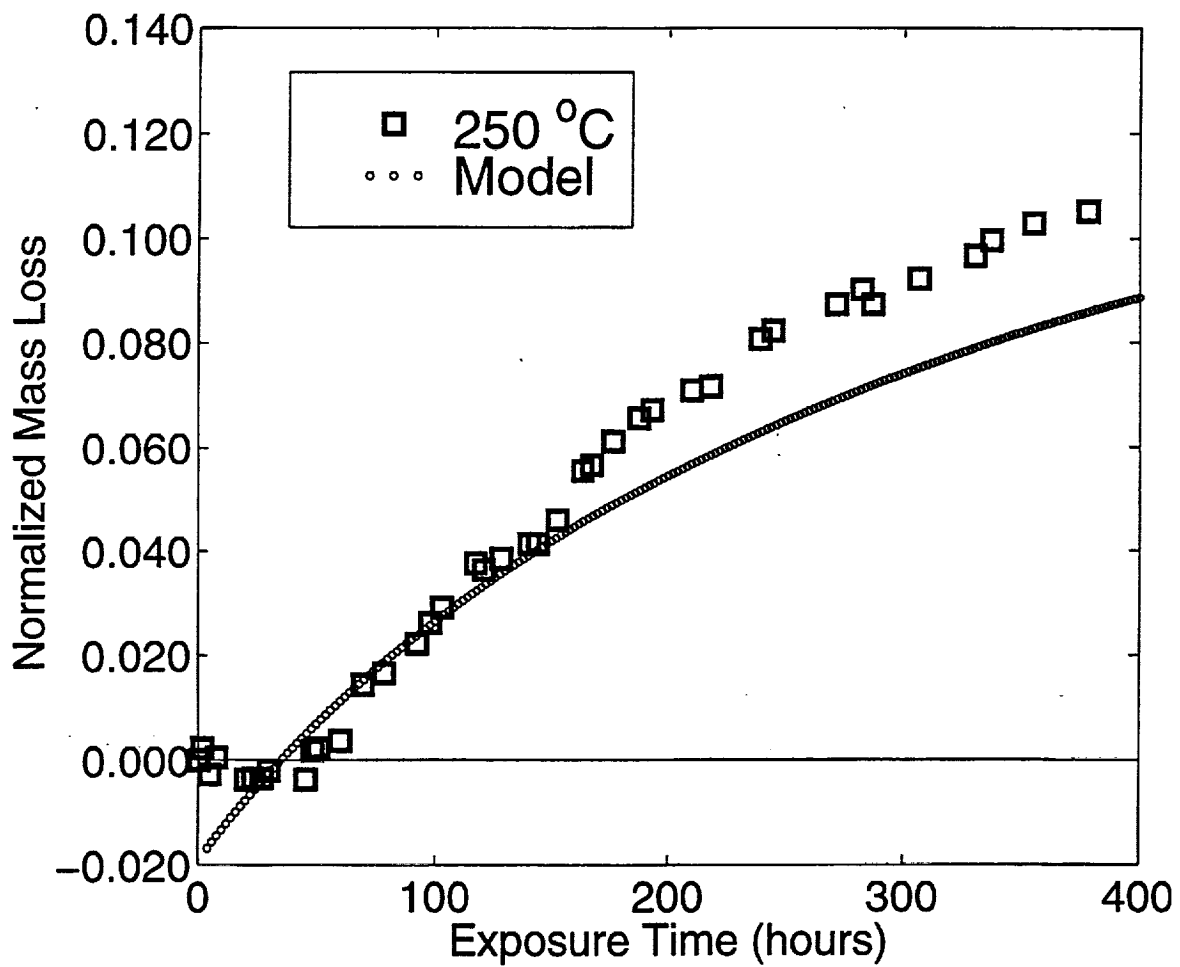
Figure 6.13   Model comparison with isothermal aging test data in air at 250˚C

60
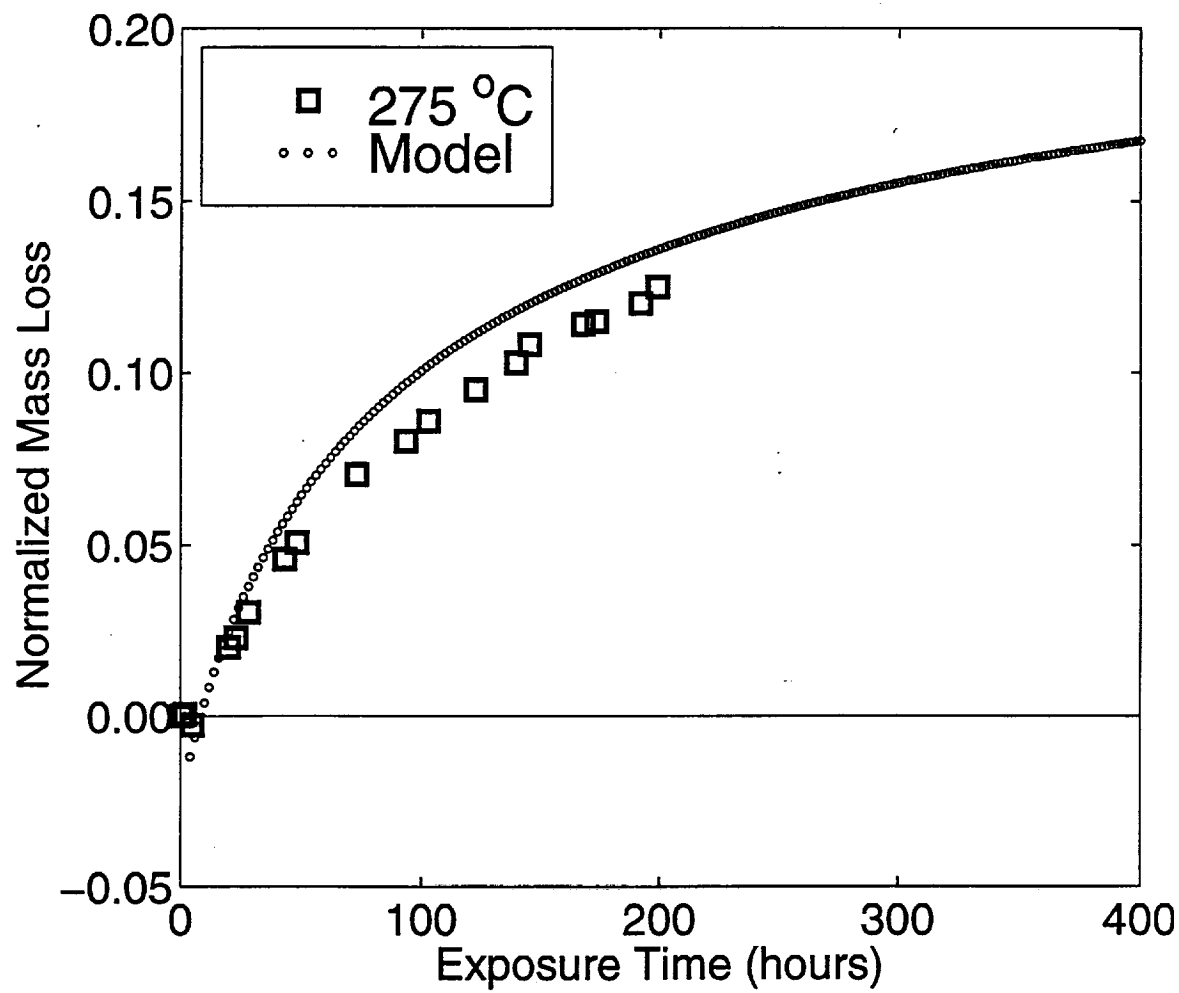
Figure 6.14   Model comparison with isothermal aging test data in air at 275°C
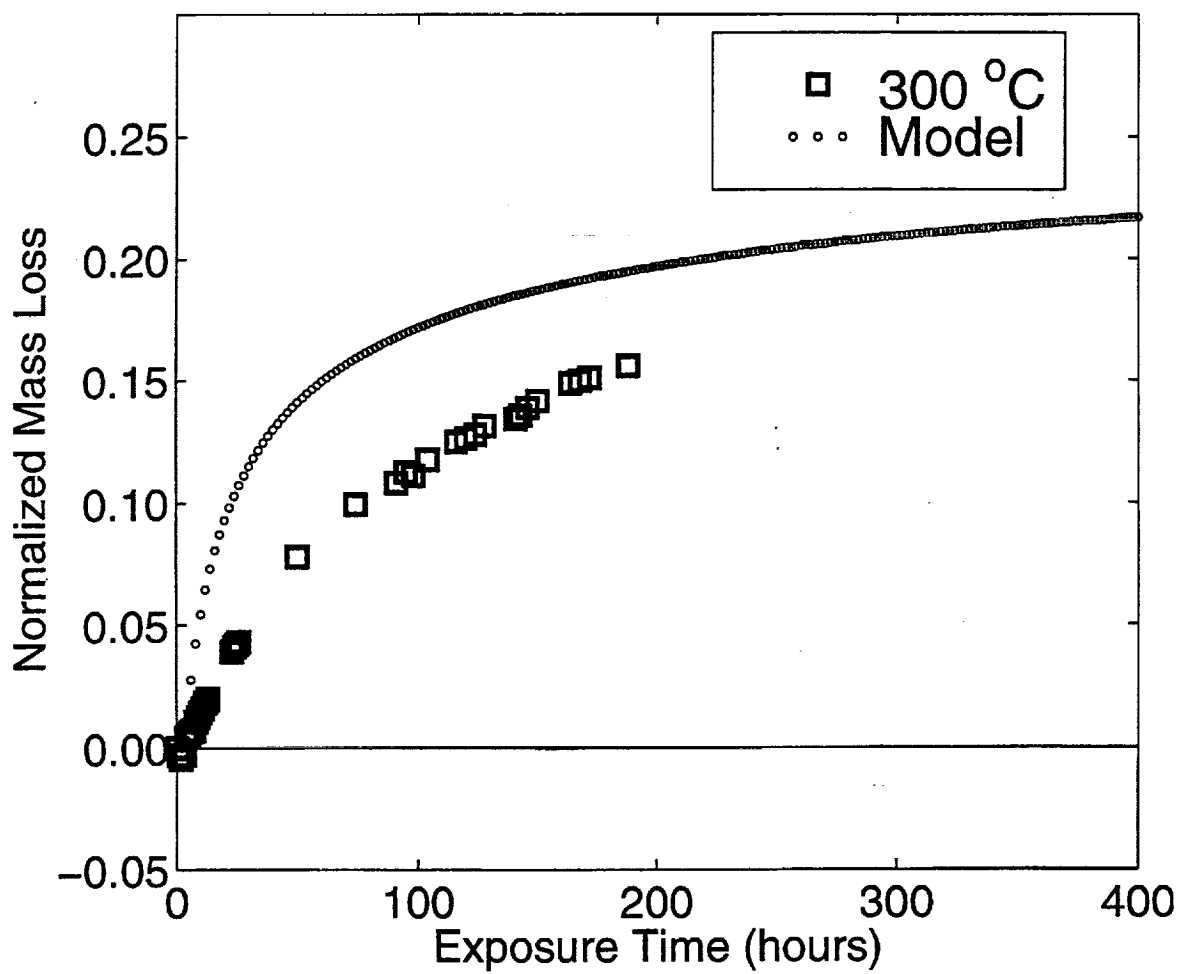
Figure 6.15   Model comparison with isothermal aging test data in air at 300°C

this is because of a transition from low temperature behavior to differing high temperature behavior.

6.2 LONG TERM ISOTHERMAL AGING TESTS IN NITROGEN

Long term aging tests in inert atmosphere were conducted at temperatures 125°C, 200°C and 300°C. Each of these tests was conducted for a much shorter duration of about 20 hours, compared to aging tests in air, because TGA tests conducted by Cunningham [1] in nitrogen had shown saturation (or near saturation) behavior in 10 hours for tests at temperatures 300°C, 340°C and 380°C. The experimental setup was modified for controlling the atmosphere in the thermocycling chamber. The details are discussed in Chapter 5. During the tests in nitrogen the sample was removed from the chamber for weight measurement. The sample was exposed to air for a period of about 30 seconds during each measurement. It was assumed that this short exposure to oxidative atmosphere would not affect the sample. However, this assumption was found to be incorrect.

At first, a test was conducted in nitrogen at 125°C to estimate the scatter and the extent of any potential moisture absorption. The measured mass loss varied from 0.0 to 1.2 mg. The lack of any trend in this data showed that the sample was not being blown away by the circulation fan or the nitrogen flow and that error due to sources such as moisture absorption was small (0.3%). The results from this test are given in the form of a normalized mass loss plot in Figure 6.16.

The results from the aging test in nitrogen conducted at 200°C and 300°C are shown in Figure 6.17 and Figure 6.18. A high initial mass loss was recorded in the test at 200°C, after which a clear mass gain trend was seen.
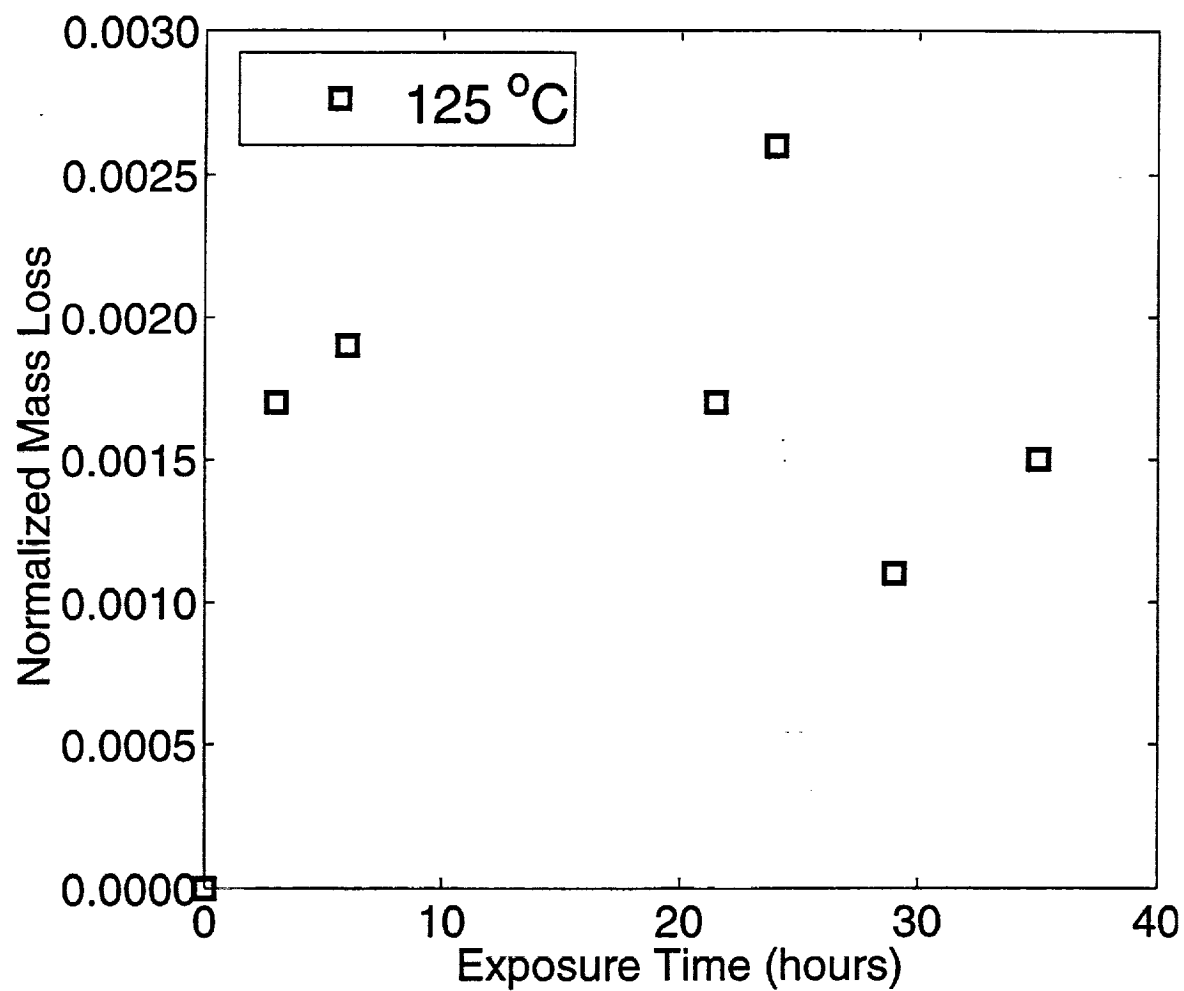
Figure 6.16   Isothermal aging test in nitrogen at 125°C
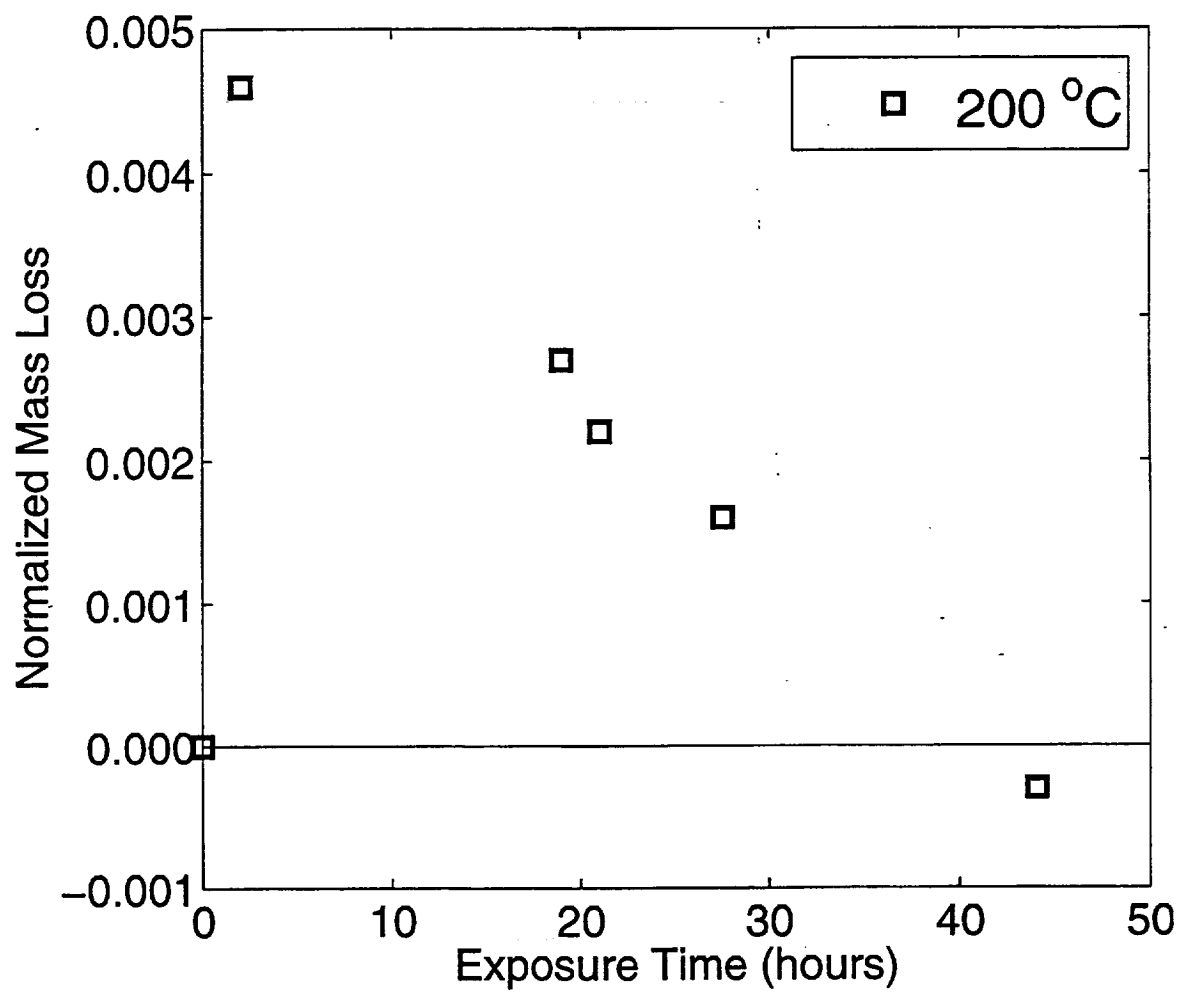
Figure 6.17   Isothermal aging test in nitrogen at 200°C
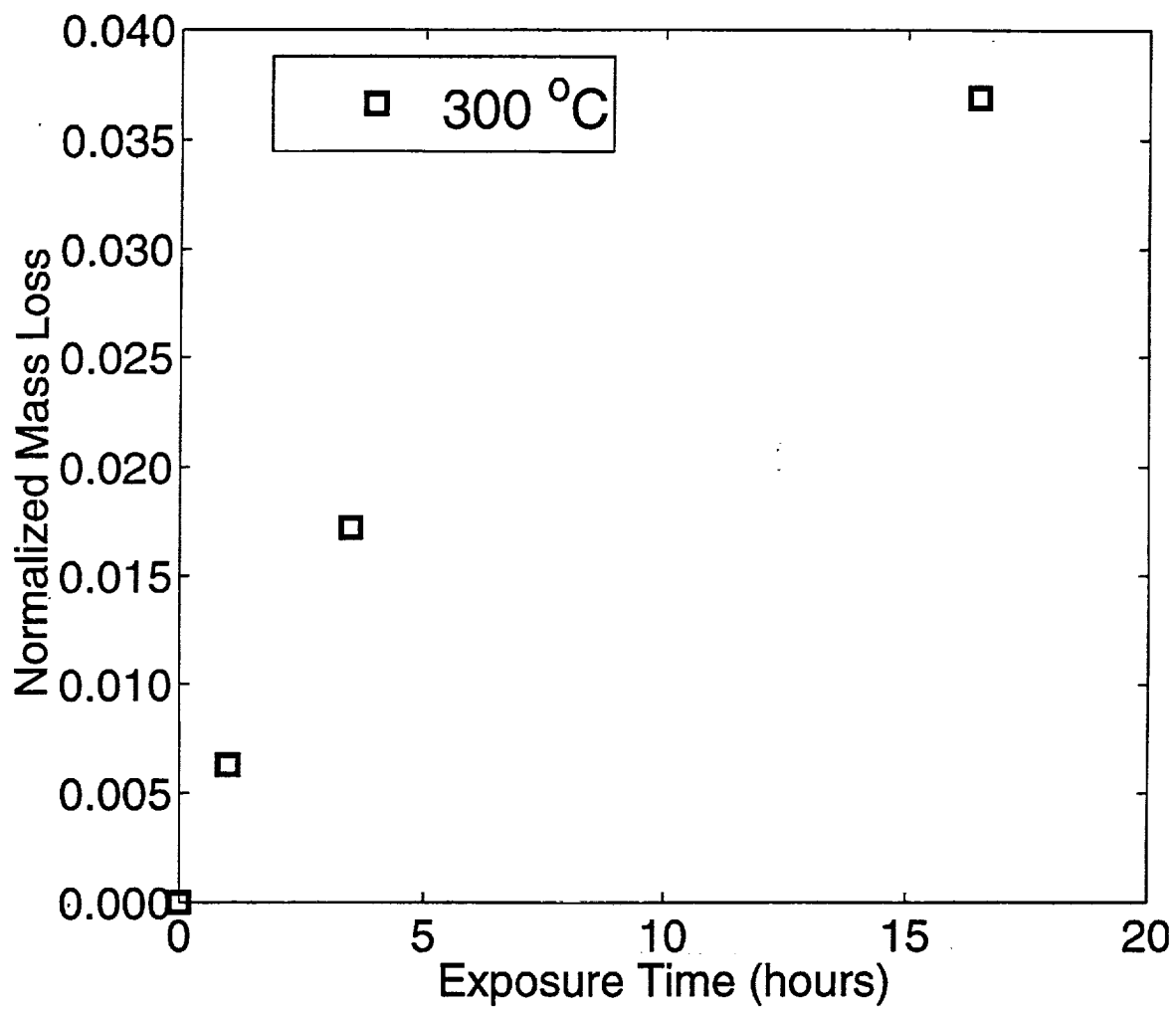
Figure 6.18   Isothermal aging test in nitrogen at 300°C

Mass gain cannot take place in an inert atmosphere. This showed that the impact of exposure to oxidative environment was significant even when such exposure was of a short duration. The test at 300°C (Figure 6.18) showed a mass loss of 1.7% after aging for 3.5 hours. The mass loss seen after 10 hours in nitrogen during isothermal TGA tests at 300°C was about 0.8% [1]. This test also showed the impact of exposure to oxidative environment. The results from these tests were therefore assumed to be invalid, and were not used for obtaining reaction coefficients.

6.3   COMBINED MODEL

A combined model was built using all the three reactions from the new model and two thermal reactions from the previous model of Cunningham [1]. The previous model had three reactions (2 thermal and 1 oxidative). The coefficients for this five reaction model are shown in Table 6.2. The new reaction model captures the behavior at low temperatures. The thermal reactions are active at higher temperatures.

The predictions using such a model were then compared with the data from dynamic TGA tests in air conducted by Cunningham [1]. The comparisons are shown in Figures 6.19 and 6.20 for two heating rates. The combined model only roughly captures the TGA data. In particular, it predicts mass addition not seen in the data.

This shows that two different models cannot be combined in such a manner to obtain a model that predicts the degradation behavior over the entire range of temperatures. The TGA data shows that at the heating rates used, no significant mass loss occurs at temperatures below 325°C. The new model worked well for temperatures only up to 275°C, and therefore cannot

Table 6.2   Coefficients for the combined five reaction model

	Mass fraction y_i	Rate constant K_i	Activation energy E_i in KJ/mol	Reaction order n_i
1	0.008	12.8×10^8	109	1.0
2	-0.026Δ	8.67×10^8	124	2.1
3	0.300	9.65×10^8	155	3.6
4ᵃ	0.160	3.12×10^{10}	182	1.6
5ᵇ	0.240	7.9×10^{12}	239	3.2

Δ   negative mass fraction represents a mass gain reaction

a, b   thermal reactions from the previous model
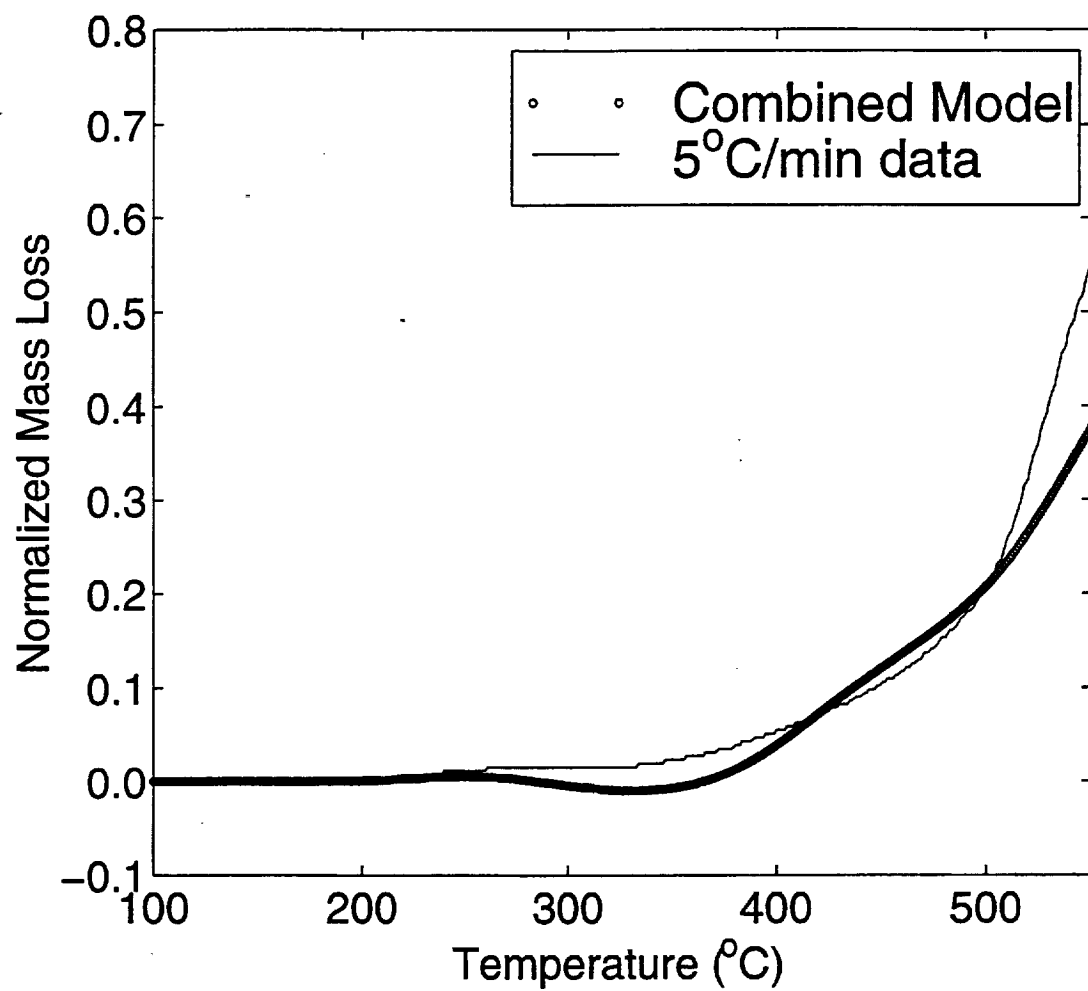
Figure 6.19   Comparison of combined model prediction with 5°C/min. heating rate TGA data in air
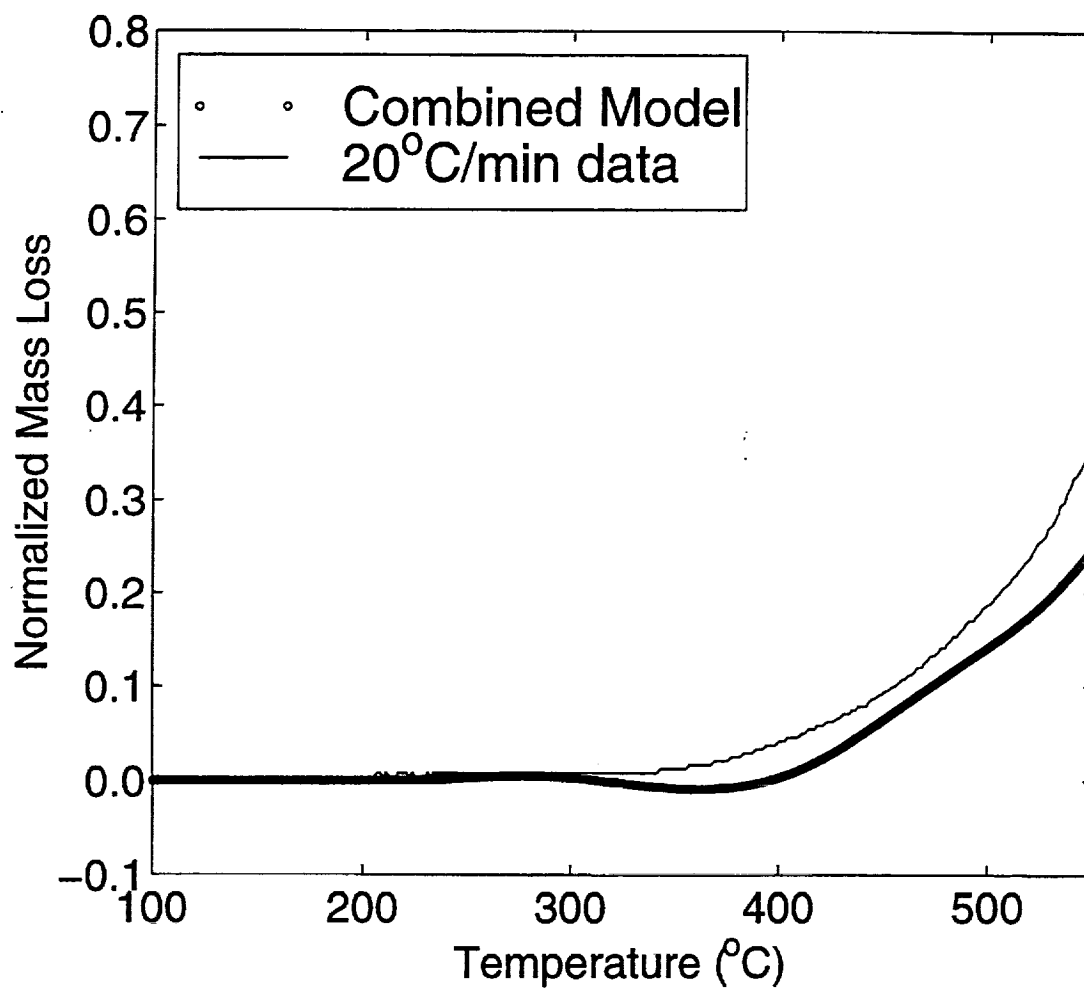
Figure 6.20   Comparison of combined model prediction with 5°C/min. heating rate TGA data in air

predict the behavior of oxidative reactions at higher temperatures. The TGA data also explains why the previous model did not capture the behavior in isothermal tests at lower temperatures. The coefficients for the model were obtained by using TGA data which did not show any degradation behavior at temperatures below 325°C.

The service conditions for PMR-15 like materials are in the range of 100 to 250°C. The present results suggest that the use of dynamic heating TGA tests is not the best method for the study of degradation behavior in this temperature region. The use of long term isothermal tests in air can capture the degradation behavior in the lower temperature region. Such long term aging tests can be conducted in a cost-effective manner as described in this thesis. Long term isothermal aging tests in air can be used successfully to characterize the material behavior for service conditions.

CHAPTER 7

CONCLUSIONS

New cost-effective experimental method

The newly developed experimental method is successful in measuring the mass loss/gain behavior and is cost-effective for long duration isothermal tests in air. The apparatus made use of a readily available thermocycling oven and a temperature controller. This method can be used for other materials.

The method, when modified for tests in an inert atmosphere, had limitations. The apparatus built from readily available components could control the atmosphere, but the intermittent exposure to air during measurements was a significant source of error. If the sample can be held in an enclosed container during measurements, this apparatus might be useful for tests in inert atmosphere.

Usefulness of long term isothermal aging tests

The data obtained from long term isothermal tests on powdered resin material is useful in material characterization. The use of powder eliminates the effects of diffusion. The mass gain behavior not seen in the previous research on this material was captured using these tests. The detection of apparent saturation behavior at some temperatures was especially useful, because it led to accurate estimation of mass fractions for the chemical reactions. Once the mass fractions were known the kinetic constants for the

Arrhenius reaction based model could be obtained with a high level of confidence.

Success of new three reaction model

The new model adequately captured the behavior in the lower temperature region (150-275°C). The in-use temperatures for PMR-15 are in the range of 150-250°C. The collected data and this model can thus be useful in the design of components using this material.

Limits of the new model

The new model could not capture the degradation behavior seen in isothermal aging at 300°C. The correlation of combined model with dynamic heating TGA test data from previous work [1] is also mediocre. The behavior at temperatures of 300°C and higher is not captured; it is suspected that this is due to fundamentally different reaction behavior at these higher temperatures.

Recommendations

The experimental method used here should be able to characterize the long term degradation behavior of high temperature resin materials. First and foremost, the isothermal aging tests are able to capture the low temperature chemistry. Also, the use of powdered specimens separates the diffusion behavior from the chemical reactions, where the use of macroscopic specimens would confound these two phenomena. This experimental method is cost-effective, reliable and accurate and is recommended for the study of other resin materials for high temperature applications.

REFERENCES

1.   Cunningham, R. A., "High Temperature Degradation Mechanisms in Polymer Matric Composites", Massachusetts Institute of Technology, S.M. Thesis, 1996.

2.   Bowles, K. J., Roberts, G. D., and Kamvouris, J. E., "Long-Term Isothermal Aging Effects on Carbon Fabric-Reinforced PMR-15 Composites: Compression Strength", NASA Technical Memorandum 107129, 1995.

3.   Kiefer, R., Yue, J. J., and Hinkley, J. A., "Kinetic Mapping of Oxidative Weight Loss in Polyimide Composites", *Journal of Advanced Materials*, Vol. 26, No. 3, 1995, pp. 55-59.

4.   Bowles, K. J., "A Thermally Modified Polymer Matrix Composite Material With Structural Integrity to 371°C", NASA Technical Memorandum 100922, 1988.

5.   Reardon, J. P., "Beyond PMR-15", *Materials Engineering*, 1992,

6.   Meador, M. A., Cavano, P. J., and Malarik, D. C., "High Temperature Polymer Matrix Composites for Extreme Environments", *Sixth Annual ASM/ESD Advanced Composites Conference*, Detroit, MI, 1990, pp. 529-539.

7.   Foch, B. J., "Integrated Degradation Models for Polymer Matrix Composites", Massachusetts Institute of Technology, S. M. Thesis, 1997.

8.   Alston, W. B., Gluyas, R. E., and Snyder, W. J., "Cyclopentadiene Evolution During Pyrolysis-Gas Chromatography of PMR Polyimides", NASA Technical Memorandum 105629, 1991.

9.   Bowles, K. J., Jayne, D., and Leonhardt, T. A., "Isothermal Aging Effects on PMR-15 Resin", *SAMPE Quarterly*, Vol. 24, No. 2, 1993, pp. 3-9.

10.   Bowles, K. J. and Nowak, G., "Thermo-Oxidative Stability Studies of Celion 6000/PMR-15 Unidirectional Composites, PMR-15, and Celion 6000 Fiber", *Journal of Composite Materials*, Vol. 22, No. 10, 1988, pp. 966-985.

11.   Bowles, K. J., "Thermo-Oxidative Stability Studies of PMR-15 Polymer Matrix Composites Reinforced with Various Continuous Fibers", *SAMPE Quarterly*, Vol. 21, No. 4, 1990, pp. 6-13.

12.   Bowles, K. J., "Effect of Fiber Reinforcements on Thermo-Oxidative Stability and Mechanical Properties of Polymer Matrix Composites", *SAMPE Quarterly*, Vol. 23, No. 3, 1992, pp. 2-12.

13.   Wong, M. S., Skontorp, A., and Wang, S. S., "Thermal Oxidation of Carbon Fibers and Carbon-Fiber Reinforced High-Temperature Polyimide

Composite at Elevated Temperatures", *ASC 9th Technical Conference*, Newark, DE, 1994, pp. 458-467.

14.   Alston, W. B., "Resin/Fiber Thermo-Oxidative Interactions in PMR Polyimide/Graphite Composites", NASA Technical Memorandum 79093, Cleveland, OH, 1979.

15.   Bowles, K. J., Jayne, D., Leonhardt, T. A., and Bors, D., "Thermal Stability Relationships Between PMR-15 Resin and Its Composites", *Journal of Advanced Materials*, Vol. 26, No. 1, 1994, pp. 23-32.

16.   Scola, D. A. a. V., J.H., "Mechanical Properties and Mechanism of the Degradation Process of 316°C Isothermally Aged Graphite Fiber/PMR-15 Composites", *Polymer Engineering and Science*, Vol. 31, No. 1, 1991, pp. 6-13.

17.   Roberts, G. D. and Lauver, R. W., "Quantitative Analysis of PMR-15 Polyimide Resin by HPLC", *Journal of Applied Polymer Science*, Vol. 33, No. 8, 1987, pp. 2893-2913.

18.   Scola, D. A. and Vontell, J. H., "High Temperature Polyimides, Chemistry and Properties", *Polymer Composites*, Vol. 9, No. 6, 1988, pp. 443-452.

19. Alston, W. B., "Characterization of PMR-15 Polyimide Resin Composition in Thermo-Oxidatively Exposed Graphite Fiber Composites", NASA Technical Memorandum 81565, 1980.

20. Pater, R. H., Whitley, K., Morgan, C., and Chang, A., "Crosslinking-Property Relationships in PMR Polyimide Composites, Part I", *Polymer Composites*, Vol. 12, No. 2, 1991, pp. 126-132.

21. Alston, W. B., "Replacement of MDA with More Oxidatively Stable Diamines in PMR-Polyimides", *High Temperature Polymer Matrix Composites*, Cleveland OH, 1985, pp. 187-205.

22. Roberts, G. D. and Vannucci, R. D., "Effect of Solution Concentration and Aging Conditions on PMR-15 Resin", *SAMPE Journal*, Vol. 22, 1986, pp. 24-28.

23. Alston, W. B., "Structure-to-Property Relationships in Addition Cured Polymers. IV - Correlations Between Thermo-Oxidative Weight Losses of Norbornenyl Cured Polyimide Resins and Their Composites", NASA Technical Memorandum 105553, 1992.

24. Cella, J. A., "Degradation and Stability of Polyimides", *Polymer Degradation and Stability*, 1992, pp. 99-110.

25.   Ansari, A. S., Turk, M. J., Alston, W. B., Frimer, A. A., and Scheiman, D. A., "TGA/FTIR Determination of Polyimide Thermal-Oxidative Degradation Kinetics", NASA preprint, 1996.

26.   Hipp, R. C., Harmon, D. M., and McClellan, P. S., "Accelerated Aging and Methodology Development for Polymeric Composite Material Systems", McDonnell Douglas Co. preprint, 1994.

27.   Hinkley, J. A. a. N., J.B., "Lifetime Extrapolation of PMR-15 and LaRC™-160 Graphite composites", *Jpurnal of Advanced Materials*, No. April, 1994,

28.   Nam, J. D. and Seferis, J. C., "Generalized Composite Degradation Kinetics for Polymeric Systems Under Isothermal and Nonisothermal Conditions", *Journal of Polymer Science: Part B: Polymer Physics*, Vol. 30, No. 5, 1992, pp. 455-463.

29.   McManus, H. L. and Chamis, C. C., "Stress and Damage in Polymer Matrix Composite Materials Due to Material Degradation at High Temperatures", NASA Technical Memorandum 4682, 1996.

30.   Tsotsis, T. K., "Thermo-Oxidative Aging of Composite Materials", *Journal of Composite Materials*, Vol. 29, No. 3, 1995, pp. 410-422.

31.   Liau, L. C. K., Yang, T.C.K. and Viwanath, D.S., "Mechanism of Degradation of Poly(Vinyl Butyral) using Thermogravimetry/Fourier

Transform Infrared Spectrometry", *Polymer Engineering and Science*, Vol. 36, No. 21, 1996, pp. 2589-2600.

32.   Jordan, K. M. a. I., J.O., "Effect of Isothermal Aging on Post-Imidization and Glass Transition Temperature of LaRC-IA Polyimide Resin", *Polymer Composites*, Vol. 18, No. June, 1997, pp. 397--404.

33.   Weisshaus, H. a. E., I., "High Temperature Properties of Ablative Composites-1", *Journal of Advanced Materials*, No. January, 1996, pp. 16-27.

34.   Boyd, J. D. and Chang, G. E. C., "Bismaleimide Composites for Advanced High-Temperature Applications", *38th International SAMPE Symposium*, Covina, CA, 1993, pp. 357-365.

35.   Maddocks, J. R., "Microcracking in Composite Laminates Under Thermal and Mechanical Loading", Massachusetts Institute of Technology, S.M. Thesis, 1995.

36.   Patekar, K. A. and McManus, H. L., "Long Term Degradation of Polyimide Composites", *8th U.S.-Japan Conference on Composite Materials*, Baltimore, MD, USA, to be presented,

37.   Patekar, K. A. and McManus, H. L., "Long Term Degradation of Polyimide Composites", 98-9, Massachusetts Institute of Technology, Cambridge, MA, USA, June, 1998.

APPENDIX A

MATLAB CODES

Files for fitting a 3 reaction model, with each reaction modeled using two constants. The inputs to be specified are xo, the initial values for these constants, and the number of iterations, options(14). The other constants specified are mass fractions, output file, input file containing the data (for 150°C data it is d150) inside the funct.m file that calculates the error between the model and the data. Outputs are the best fit constants and the error calculated.

```
%      File t2.m
% A constrained optimization approach to curve-fitting
% Intermediate step curve-fitting using only two constants per reaction
% The C constant is multiplied by 1e-7 inside the funct.m evaluation
tic;
x0=[1 2 3.2; 800 3 .0005];
options(1)=1;              % display paramters
options(14)=100;          % Max number of function evaluations
% Lower and upper limits on variables [ reaction order ; C ]
vlb=[ 0.8 1.9 3.16; 0.1 0.1 0.001];
vub=[ 1.2 2.3 3.24; 50000 5000 1];
% Matlab function for doing the optimization
[best]=constr('funct',x0,options,vlb,vub);
[error,g,yi,number,data,o_file]=funct(best);
[model]=sim_reaction(best(2,:),yi,best(1,:),data,number);
% generate a curve for the reaction_order numbers
plotdata(data,'ro',1);
hold on;
plotdata(model,'k-',0);
%printing output to a file specified inside funct.m
fprintf(o_file,'%9.3E  ',best(2,:));
fprintf(o_file,'%6.5f ',yi);
fprintf(o_file,'%4.2f ',best(1,:));
fprintf(o_file,'%9.3E ',error);
fprintf(o_file,'\n');
fclose('all');
toc; % for measuring the time taken by the code to run
% end of t2.m
```

```
% ***************************************************************
% sim_reaction.m
function[model] =sim_reaction(C, yi, ni, data, number)
% This is a function for simulating multiple reactions and
% gives the total alpha


% Initialization and data set size determiniation etc.
deltat=1800;
r=size(data,1);
N=data(r,1);
Nu=N*(3600/deltat);
alpha(Nu,number)=0;
dalphadt(Nu,number)=0;

% Simulating the reactions using a finite difference scheme

for j=1:number,

    for i=1:Nu,
      if alpha(i,j) <= 1 &  alpha(i,j) >=0

% $$$$$$$ Factor of 1e-7 included in next line

        dalphadt(i,j)=C(j)*1e-7*(1-alpha(i,j))^ni(j);
        alpha(i+1,j)=alpha(i,j)+dalphadt(i,j)*deltat;
        if alpha(i+1,j) > 1 alpha(i+1,j)=1; end
        if alpha(i+1,j) < 0 alpha(i+1,j)=0; end

      elseif alpha(i,j) < 0
        dalphadt(i,j)=0;
        alpha(i+1,j)=0;
      elseif alpha(i,j) > 1
        dalphadt(i,j)=0;
        alpha(i+1,j)=1;

      end

      t(i)=i*(deltat/3600);

    end

end

alpha_T(1:Nu,1)=0;

% Sum the reactions metrics weighted by their mass fractions
for j=1:number;
alpha_T=alpha_T+yi(j)*alpha(1:Nu,j);
end
model(Nu,2)=0;
model(1:Nu,1)=[t'];
model(1:Nu,2)=[alpha_T];
```

```
% end of sim_reaction.m
% ***************************************************************

% funct.m

% Defining a function that generates an error estimate

function [error,g,varargout] = funct(x)

% getting the data file of interest and setting the output file
load d200;
data=d200;
o_file='200.opt';


% Mass fractions
yi=[0.008 -0.026 0.35];

% Numer of reactions used in the model
number=3;

[model_pred]=sim_reaction(x(2,:),yi,x(1,:),data,number);
error=model_error(model_pred,data);


% It is necessary to specify these constraints

%g(1)=-x(1,1);
%g(2)=-x(1,2);
%g(3)=-x(1,3);
%g(4)=-x(2,1);
%g(5)=-x(2,2);
%g(6)=-x(2,3);

% error has to be less than 1e-4
g(1)=error-1e-4;


varargout{1}=yi;
varargout{2}=number;
varargout{3}=data;
varargout{4}=o_file;

% end of funct.m

% ***************************************************************

% model_error.m
% Calculates the least sq. error between the model predictions
% and the data
function[terr]=model_error(model,data)
```

```
r=size(data,1);
deltat=1800;
err=0;
terr=0;
dum=0;

for i=1:10,

        dum=data(i,1)*(3600/deltat);
        err=sqrt((data(i,2)-model(dum,2))^2);
        terr=terr+err;

end

for i=11:r,
        dum=data(i,1)*(3600/deltat);
        err=sqrt((data(i,2)-model(dum,2))^2);
        terr=terr+ err;
end

terr=terr/r;

% end of model_error.m

% ****************************************************************
% plotdata.m

function[plt] = plotdata(data,x,type)
r=size(data,1);   %  Get number of rows for the data matrix

% type 1 for data and type 0 for model
if type == 1
  plot(data(1:r,1),data(1:r,2),x,'MarkerSize',10,'LineWidth',2.0);
elseif type== 0
  plot(data(1:r,1),data(1:r,2),x,'MarkerSize',3,'LineWidth',0.5);
end

% needed only for writing the axis labels
gca;
set(gca,'FontSize',18,'FontName','Helvetica','XLim',[0 700]);
xlabel('Exposure Time (hours)');
ylabel('Normalized Mass Loss ');
% setting the figure position on paper
%gcf;
%set(gcf,'PaperPosition',[1.25 2 4 4.5]);
%to make axis print in figure -- either make figure bigger, or...
axpos = get(gca,'position');
set(gca,'position',axpos+[0 .03 0 -.03]);

% end of plotdata.m
%****************************************************************
```

Files for doing the full scale optimization using all the 3 constants to specify each reaction. Here, the inputs are all the constants for the three reactions, the ranges in which they should be optimized, and the number of iterations to be carried out. All these are specified inside the file bigt.m which starts the optimization.

```
% bigt.m
% A constrained optimization approach to finding reaction coefficients
% Variables: reaction order, rate constant K, activation energy Ea
% Use of scaling factors to facilitate solution search
% for K it is 1e10
% for Ea it is 1e4
tic;
for i=1:3, figure(i); clf; end
% x0 is specified as, reaction orders, rate constants and then activation energy
% for all the 3 reactions
x0=[1.0 2 3.3; 0.10 0.10 0.10; 11  12.4 15.6];
options(1)=1;              % display paramters
options(3)=1e-4;           % termination tolerance for f
m=100;
options(14)=m; % Max number of function evaluations
% Lower and upper limits on variables [ reaction order ; K, Ea ]
vlb=[ 0.9 1.0 2.5; 0.07 0.07 0.07; 10 11 14.8 ];
vub=[ 1.1 2.1 4; 0.25 0.25 0.25; 12 14 17];
[best]=constr('bigfun',x0,options,vlb,vub);
[terror,g,yi,number]=bigfun(best);
% Generating curves and model fits for all data sets
s=['d150' ; 'd175'; 'd200' ; 'd225' ; 'd250' ; 'd275' ; 'd300'];
for i=1:7,
T=125+273+i*25;
a=s(i,:);
load(a);
data=eval(a);
[model]=simr(best(2,:),T,best(3,:),yi,best(1,:),data,number);
if i==1
        figure(1);
plotdata(data,'ks',1);
hold on;
plotdata(model,'ro',0);
elseif i==2
        figure(1);
plotdata(data,'kd',1);
hold on;
plotdata(model,'ro',0);
elseif i==3
        figure(2);
plotdata(data,'ks',1);
```

```
hold on;
plotdata(model,'ro',0);
elseif i==4
        figure(2);
plotdata(data,'kv',1);
hold on;
plotdata(model,'ro',0);
elseif i==5
        figure(3);
plotdata(data,'kd',1);
hold on;
plotdata(model,'ro',0);
elseif i==6
        figure(3);
plotdata(data,'ks',1);
hold on;
plotdata(model,'ro',0);
elseif i==7
        figure(3);
plotdata(data,'kv',1);
hold on;
plotdata(model,'ro',0);
end
end
o_file='total.pt';
fprintf(o_file,'%9.3E ',best(2,:));
fprintf(o_file,'%5.3f ',yi);
fprintf(o_file,'%4.2f ',best(1,:));
fprintf(o_file,'%9.3f ',best(3,:));
fprintf(o_file,'%9.3E ',terror);
fprintf(o_file,'%3i',m);
fprintf(o_file,'\n');
fclose('all');
toc; % for measureing the time taken by the code to run
% end of bigt.m

% ***************************************************************************
% bigfun.m
% A function to generate an error function over all the data sets
function [terror, g, varargout] = bigfun(x)
% Mass fractions
yi=[0.008 -0.026 0.20];
% Numer of reactions used in the model
number=3;
error=0;
terror=0;
T=0;
s=['d150' ; 'd175'; 'd200' ; 'd225' ; 'd250' ; 'd275' ; 'd300'];
% A mean of the data points is used as a scaling factor
scale_factor=[0.0046 0.0118 0.0092 0.015 0.0678 0.0659 0.0712];
% Just to give more weightage to d300 data
scale_factor(7)=scale_factor(7)/1.5;
for i=1:7,
```

```
a=s(i,:);
load(a);
data=eval(a);
T=273+125+i*25;
[model_pred]=simr(x(2,:),T,x(3,:),yi,x(1,:),data,number);
error=model_error(model_pred,data);
terror=(error/scale_factor(i))+terror;
end
% Total error has to be less than 1e-4
g(1)=terror-1e-6;
varargout{1}=yi;
varargout{2}=number;
% end of bigfun.m


% ********************************************************

% simr.m
% A function to implement the model
function[model] =simr(K,T,Ea, yi, ni, data, number)
% This is a function for simulating multiple reactions and
% gives the total alpha which make use of a full model using activation
% energy and temperature
% Initialization and data set size determiniation etc.
deltat=1800;
r=size(data,1);
N=data(r,1);
Nu=N*(3600/deltat);
alpha(1:Nu,1:number)=0;
dalphadt(1:Nu,1:number)=0;
R=8.314;
dum1=0;
dum2=0;
dum3=0;
% Calculating the reaction coeff
for m=1:number,
        dum1=-Ea(m)*1e4;
        dum2=R*T;
        dum3=exp(dum1/dum2);
        C(m)=K(m)*1e10*dum3;
end
% Simulating the reactions using a finite difference scheme
for j=1:number,
    for i=1:Nu,
      if alpha(i,j) <= 1 &  alpha(i,j) >=0
dalphadt(i,j)=C(j)*(1-alpha(i,j))^ni(j);
        alpha(i+1,j)=alpha(i,j)+dalphadt(i,j)*deltat;
        if alpha(i+1,j) > 1 alpha(i+1,j)=1; end
        if alpha(i+1,j) < 0 alpha(i+1,j)=0; end
      elseif alpha(i,j) < 0
        dalphadt(i,j)=0;
        alpha(i+1,j)=0;
      elseif alpha(i,j) > 1
        dalphadt(i,j)=0;
```

```
         alpha(i+1,j)=1;
         end
      t(i)=i*(deltat/3600);
    end
end
alpha_T(1:Nu,1)=0;
% Sum the reactions metrics weighted by their mass fractions
for j=1:number;
alpha_T=alpha_T+yi(j)*alpha(1:Nu,j);
end
model(Nu,2)=0;
model(1:Nu,1)=[t'];
model(1:Nu,2)=[alpha_T];
% end of simr.m


% ******************************************************************************

% model_error.m
% Calculates the least sq. error between the model predictions
% and the data
function[terr]=model_error(model,data)
r=size(data,1);
deltat=1800;
err=0;
terr=0;
dum=0;
for i=1:10,
        dum=data(i,1)*(3600/deltat);
        err=sqrt((data(i,2)-model(dum,2))^2);
        terr=terr+err;
end
for i=11:r,
        dum=data(i,1)*(3600/deltat);
        err=sqrt((data(i,2)-model(dum,2))^2);
        terr=terr+ err;
end
terr=terr/r; % dividing th error by the number of points of data
% end of model_error.m
% A functions to generate curves by loading the data and plotting it appropriately
% A function to plot different sets of data
% fig.m
a=char('d125','d150','d175','d200','d225','d250','d275','d300');
s=char('125 ^oC','150 ^oC','175 ^oC','200 ^oC','225 ^oC','250 ^oC','275 ^oC','300 ^oC');
% Specify a number between 1 and 8 to obtaint the appropriate figure
m=1;
figure(1);
for i=m,
        load(a(i,:));
        data=eval(a(i,:));
        r=size(data,1);
        plot(data(1:r,1),data(1:r,2),'ks','MarkerSize',10,'LineWidth',2.0);
        hold on
end
```

```
ax1=gca;
set(gca,'FontSize',18,'FontName','Helvetica');
%set(gca,'FontSize',18,'FontName','Helvetica','XLim',[0 200],'YLim',[-0.0020 0.002]);
xlabel('Exposure Time (hours)');
ylabel('Normalized Mass Loss ');
% To put a line at [0 0]
xlim = get(ax1,'xlim');
l = line(xlim,[0 0],'color','k','parent',ax1);
% To get formatted ticklabels
yt= 0:0.005:.04 ; % ticks
yl = sprintf('%.3f|',yt); %tick label with extra |
yl(end) = []; %without extra |
set(gca,'ylim',[min(yt) max(yt)],'yticklabel',yl); %limit and label
%to help with the legend modification, keep track of new lines
lbefore = findobj(gcf,'type','line');
ax=gca;
%to put up several tickmarks in the pseudo-legend
%you need one symbol per line
%legend('150 ^oC','175 ^oC','200 ^oC','225 ^oC',0);
legend(s(m,:),1);
%make marks in legend for each entry
lafter = findobj(gcf,'type','line');
lnew = setdiff(lafter,lbefore);
for k=1:length(lnew)
  ly = get(lnew(k),'ydata');
  set(lnew(k),'xdata',.3,'ydata',ly(1));
end
gcf;
%set(gcf,'PaperPosition',[1.5 2 5.5 4]);
set(gca,'position',[0.20 0.12 0.675 0.815])


% ************************************************************
% A function to obtain model comparison with data plots
% Generating curves and model fits for all data sets
best=[1.01  2.04  3.49 ;9.214E-02 1.044E-01 1.337E-01;11.015 12.499 15.40];
yi=[ 0.008 -0.026 0.30];
number=3;
s=['d150' ; 'd175'; 'd200' ; 'd225' ; 'd250' ; 'd275' ; 'd300'];
m=7;
for i=m,
        a=s(i,:);
        load(a);
        data=eval(a);
        figure(1);
        plotdata(data,'ks',1);
        hold on;
end
for i=m,
        T=125+273+i*25;
        a=s(i,:);
        load(a);
        data=eval(a);
        [model]=plotsimr(best(2,:),T,best(3,:),yi,best(1,:),data,number);
```

```
        plotdata(model,'ro',0);
end
ax1=gca;
%set(gca,'FontSize',12,'FontName','Times','XLim',[0 400],'YLim',[-0.020 0.01]);
set(gca,'FontSize',18,'FontName','Helvetica','XLim',[0 400]);
%to help with the legend modification, keep track of new lines
lbefore = findobj(gcf,'type','line');
%to put up several tickmarks in the pseudo-legend
%you need one symbol per line
legend('300 ^oC','Model',0);
%make 1 marks in legend for each entry
lafter = findobj(gcf,'type','line');
lnew = setdiff(lafter,lbefore);
for k=1:length(lnew),
  ly = get(lnew(k),'ydata');
  set(lnew(k),'xdata',.3,'ydata',ly(1,1));
end
for k=length(lnew),
        ly=get(lnew(k),'ydata');
        set(lnew(k),'xdata',.23:0.07:0.37,'ydata',ones(1,3)*ly(1));
end
% To put a line at [0 0]
xlim=get(ax1,'xlim');
l=line(xlim,[0 0],'color','k','parent',ax1);
% to put in formatted tick labels
yt3 = -0.05:0.05:.30; %ticks
yl3 = sprintf('%.2f| ',yt3); %tick label with extra |
yl3(end) = []; %without extra |
set(gca,'ylim',[min(yt3) max(yt3)],'yticklabel',yl3); %limit and label
gcf;
%set(gcf,'PaperPosition',[1.5 2 5.5 4]);
set(gca,'position',[0.20 0.12 0.675 0.805])


% ***********************************************
% File plotsimr.m
% A file to generate the model values specifically for the curves
function[model] =plotsimr(K,T,Ea, yi, ni, data, number)
% This is a function for simulating multiple reactions and
% gives the total alpha which make use of a full model using activation
% energy and temperature
% Initialization and data set size determiniation etc.
deltat=7200;
%r=size(data,1);
%N=data(r,1);
% Plot for 400 hours
Nu=200;
alpha(1:Nu,1:number)=0;
dalphadt(1:Nu,1:number)=0;
R=8.314;
dum1=0;
dum2=0;
dum3=0;
% Calculating the reaction coeff
```

```
for m=1:number,
        dum1=-Ea(m)*1e4;
        dum2=R*T;
        dum3=exp(dum1/dum2);
        C(m)=K(m)*1e10*dum3;
end
% Simulating the reactions using a finite difference scheme
for j=1:number,
    for i=1:Nu,
      if alpha(i,j) <= 1 &  alpha(i,j) >=0
        dalphadt(i,j)=C(j)*(1-alpha(i,j))^ni(j);
        alpha(i+1,j)=alpha(i,j)+dalphadt(i,j)*deltat;
        if alpha(i+1,j) > 1 alpha(i+1,j)=1; end
        if alpha(i+1,j) < 0 alpha(i+1,j)=0; end
      elseif alpha(i,j) < 0
        dalphadt(i,j)=0;
        alpha(i+1,j)=0;
      elseif alpha(i,j) > 1
        dalphadt(i,j)=0;
        alpha(i+1,j)=1;
      end
      t(i)=i*(deltat/3600);
%        t(i)=i*0.5;
    end
end
alpha_T(1:Nu,1)=0;
% Sum the reactions metrics weighted by their mass fractions
for j=1:number;
alpha_T=alpha_T+yi(j)*alpha(1:Nu,j);
end
model(Nu,2)=0;
model(1:Nu,1)=[t'];
model(1:Nu,2)=[alpha_T];
```

APPENDIX B

ISOTHERMAL AGING IN AIR TEST DATA

In all the tables given here, Time is in hours, Sample Mass and Mass loss are in grams. Normalized Mass Loss is given in the last column.

Table B.1   Data for test at 125°C

Time	Sample Mass	Mass loss	Normalized
0.0	0.6438	0.0000	0.0000
2.0	0.6429	0.0009	0.0014
4.0	0.6428	0.0010	0.0016
6.0	0.6429	0.0009	0.0014
19.0	0.6441	-0.0003	-0.0005
21.0	0.6443	-0.0005	-0.0008
23.0	0.6433	0.0005	0.0008
50.0	0.6432	0.0006	0.0009
52.0	0.6433	0.0005	0.0008
56.0	0.6439	-0.0001	-0.0002
74.0	0.6428	0.0010	0.0016
76.0	0.6439	-0.0001	-0.0002
79.5	0.6440	-0.0002	-0.0003
97.0	0.6437	0.0001	0.0002
99.5	0.6440	-0.0002	-0.0003
122.0	0.6443	-0.0005	-0.0008
124.0	0.6438	0.0000	0.0000
127.0	0.6438	0.0000	0.0000
130.5	0.6431	0.0007	0.0011
142.0	0.6436	0.0002	0.0003
146.0	0.6440	-0.0002	-0.0003
148.0	0.6449	-0.0011	-0.0017
171.0	0.6445	-0.0007	-0.0011
191.0	0.6438	0.0000	0.0000
194.0	0.6441	-0.0003	-0.0005
214.0	0.6446	-0.0008	-0.0012

Table B.2 Data for test at 150°C

Time	Sample Mass	Mass Loss	Normalized
0.0	0.7472	0.0000	0.0000
1.0	0.7458	0.0014	0.0019
26.0	0.7427	0.0045	0.0060
30.5	0.7420	0.0052	0.0070
50.5	0.7430	0.0042	0.0056
54.5	0.7418	0.0054	0.0072
65.5	0.7444	0.0028	0.0037
69.0	0.7430	0.0042	0.0056
73.0	0.7436	0.0036	0.0048
77.0	0.7443	0.0029	0.0039
92.5	0.7439	0.0033	0.0044
96.0	0.7435	0.0037	0.0050
101.0	0.7429	0.0043	0.0058
115.0	0.7437	0.0035	0.0047
119.0	0.7441	0.0031	0.0041
142.0	0.7441	0.0031	0.0041
154.0	0.7440	0.0032	0.0043

Table B.3   Data for test at 175°C

Time	Sample Mass	Mass Loss	Normalized
0.0	0.6604	0.0000	0.0000
1.5	0.6590	0.0014	0.0021
23.0	0.6585	0.0019	0.0029
33.5	0.6650	-0.0046	-0.0070
60.0	0.6642	-0.0038	-0.0058
64.0	0.6677	-0.0073	-0.0111
86.0	0.6653	-0.0049	-0.0074
107.0	0.6674	-0.0070	-0.0106
116.5	0.6662	-0.0058	-0.0088
129.5	0.6679	-0.0075	-0.0114
154.5	0.6685	-0.0081	-0.0123
162.0	0.6685	-0.0081	-0.0123
177.0	0.6666	-0.0062	-0.0094
184.0	0.6679	-0.0075	-0.0114
202.0	0.6679	-0.0075	-0.0114
212.0	0.6674	-0.0070	-0.0106
240.0	0.6701	-0.0097	-0.0147
283.5	0.6694	-0.0090	-0.0136
307.5	0.6707	-0.0103	-0.0156
320.5	0.6708	-0.0104	-0.0157
333.0	0.6678	-0.0074	-0.0112
360.0	0.6709	-0.0105	-0.0159
392.0	0.6712	-0.0108	-0.0164
407.0	0.6713	-0.0109	-0.0165
461.0	0.6718	-0.0114	-0.0173
486.0	0.6711	-0.0107	-0.0162
502.0	0.6714	-0.0110	-0.0167
525.0	0.6719	-0.0115	-0.0174
552.5	0.6723	-0.0119	-0.0180
573.5	0.6723	-0.0119	-0.0180
602.5	0.6717	-0.0113	-0.0171

Table B.4   Data for test at 200°C

Time	Sample Mass	Mass Loss	Normalized
0.0	0.5893	0.0000	0.0000
2.0	0.5875	0.0018	0.0031
4.0	0.5889	0.0004	0.0007
6.0	0.5885	0.0008	0.0014
8.0	0.5891	0.0002	0.0003
10.0	0.5887	0.0006	0.0010
21.0	0.5916	-0.0023	-0.0039
23.0	0.5915	-0.0022	-0.0037
25.5	0.5915	-0.0022	-0.0037
29.0	0.5914	-0.0021	-0.0036
31.0	0.5914	-0.0021	-0.0036
34.0	0.5921	-0.0028	-0.0048
45.5	0.5932	-0.0039	-0.0066
48.0	0.5931	-0.0038	-0.0064
50.0	0.5936	-0.0043	-0.0073
57.0	0.5942	-0.0049	-0.0083
68.5	0.5941	-0.0048	-0.0081
72.0	0.5947	-0.0054	-0.0092
76.5	0.5943	-0.0050	-0.0085
82.0	0.5941	-0.0048	-0.0081
94.5	0.5959	-0.0066	-0.0112
96.0	0.5946	-0.0053	-0.0090
101.5	0.5952	-0.0059	-0.0100
104.0	0.5955	-0.0062	-0.0105
120.0	0.5952	-0.0059	-0.0100
146.0	0.5961	-0.0068	-0.0115
150.0	0.5969	-0.0076	-0.0129
152.0	0.5965	-0.0072	-0.0122
166.0	0.5963	-0.0070	-0.0119
169.0	0.5964	-0.0071	-0.0120
172.0	0.5970	-0.0077	-0.0131
188.0	0.5972	-0.0079	-0.0134
191.0	0.5975	-0.0082	-0.0139
193.0	0.5981	-0.0088	-0.0149
196.5	0.5981	-0.0088	-0.0149
200.0	0.5969	-0.0076	-0.0129
202.0	0.5958	-0.0065	-0.0110
212.0	0.5980	-0.0087	-0.0148
215.5	0.5961	-0.0068	-0.0115
220.5	0.5966	-0.0073	-0.0124
223.0	0.5967	-0.0074	-0.0126
226.0	0.5964	-0.0071	-0.0120
240.0	0.5969	-0.0076	-0.0129
242.0	0.5966	-0.0073	-0.0124
244.0	0.5977	-0.0084	-0.0143
249.5	0.5963	-0.0070	-0.0119

Table B.4 (contd.)

Time	Sample Mass	Mass Loss	Normalized
268.0	0.5978	-0.0085	-0.0144
289.0	0.5968	-0.0075	-0.0127
315.0	0.5964	-0.0071	-0.0120
320.0	0.5962	-0.0069	-0.0117
333.0	0.5973	-0.0080	-0.0136
338.0	0.5966	-0.0073	-0.0124
345.0	0.5966	-0.0073	-0.0124

Table B.5   Data for test at 225°C

Time	Sample Mass	Mass Loss	Normalized
0.0	0.6588	0.0000	0.0000
2.5	0.6598	-0.0010	-0.0015
4.0	0.6592	-0.0004	-0.0006
16.0	0.6659	-0.0071	-0.0108
18.5	0.6658	-0.0070	-0.0106
22.0	0.6658	-0.0070	-0.0106
41.0	0.6670	-0.0082	-0.0124
44.0	0.6669	-0.0081	-0.0123
64.5	0.6665	-0.0077	-0.0117
68.5	0.6659	-0.0071	-0.0108
95.5	0.6650	-0.0062	-0.0094
116.5	0.6629	-0.0041	-0.0062
137.0	0.6620	-0.0032	-0.0049
141.0	0.6622	-0.0034	-0.0052
162.5	0.6611	-0.0023	-0.0035
168.0	0.6599	-0.0011	-0.0017
188.0	0.6590	-0.0002	-0.0003
219.5	0.6570	0.0018	0.0027
226.0	0.6556	0.0032	0.0049
251.0	0.6546	0.0042	0.0064
271.5	0.6514	0.0074	0.0112
298.5	0.6496	0.0092	0.0140
320.0	0.6482	0.0106	0.0161
342.0	0.6463	0.0125	0.0190
364.0	0.6446	0.0142	0.0216

Table B.6   Data for test at 250°C

Time	Sample Mass	Mass Loss	Normalized
0.0	0.5639	0.0000	0.0000
2.0	0.5626	0.0013	0.0023
5.0	0.5654	-0.0015	-0.0027
8.0	0.5636	0.0003	0.0005
20.5	0.5660	-0.0021	-0.0037
23.5	0.5659	-0.0020	-0.0035
27.0	0.5659	-0.0020	-0.0035
30.0	0.5650	-0.0011	-0.0020
45.5	0.5660	-0.0021	-0.0037
48.5	0.5629	0.0010	0.0018
51.0	0.5626	0.0013	0.0023
60.0	0.5618	0.0021	0.0037
69.5	0.5558	0.0081	0.0144
78.5	0.5546	0.0093	0.0165
92.5	0.5514	0.0125	0.0222
98.0	0.5491	0.0148	0.0262
103.0	0.5475	0.0164	0.0291
117.5	0.5427	0.0212	0.0376
121.0	0.5434	0.0205	0.0364
125.0	0.5426	0.0213	0.0378
128.5	0.5422	0.0217	0.0385
140.5	0.5406	0.0233	0.0413
144.0	0.5406	0.0233	0.0413
148.0	0.5392	0.0247	0.0438
152.5	0.5380	0.0259	0.0459
163.5	0.5326	0.0313	0.0555
167.5	0.5320	0.0319	0.0566
171.5	0.5308	0.0331	0.0587
176.5	0.5294	0.0345	0.0612
187.5	0.5269	0.0370	0.0656
193.0	0.5260	0.0379	0.0672
210.0	0.5239	0.0400	0.0709
214.0	0.5245	0.0394	0.0699
218.0	0.5235	0.0404	0.0716
239.0	0.5184	0.0455	0.0807
244.5	0.5175	0.0464	0.0823
271.5	0.5146	0.0493	0.0874
282.5	0.5130	0.0509	0.0903
287.0	0.5146	0.0493	0.0874
306.5	0.5118	0.0521	0.0924
311.5	0.5115	0.0524	0.0929
330.5	0.5093	0.0546	0.0968
337.5	0.5077	0.0562	0.0997
355.5	0.5059	0.0580	0.1029

Table B.6   (contd.)

Time	Sample Mass	Mass Loss	Normalized
378.5	0.5046	0.0593	0.1052
409.5	0.5024	0.0615	0.1091
431.5	0.4995	0.0644	0.1142
449.5	0.4995	0.0644	0.1142
473.0	0.4982	0.0657	0.1165
501.0	0.4944	0.0695	0.1232
524.0	0.4940	0.0699	0.1240
541.5	0.4938	0.0701	0.1243
572.0	0.4896	0.0743	0.1318
596.0	0.4898	0.0741	0.1314
622.5	0.4881	0.0758	0.1344
637.0	0.4873	0.0766	0.1358
665.0	0.4861	0.0778	0.1380
688.0	0.4840	0.0799	0.1417
732.0	0.4828	0.0811	0.1438
781.0	0.4812	0.0827	0.1467
806.0	0.4789	0.0850	0.1507
829.0	0.4774	0.0865	0.1534
859.5	0.4774	0.0865	0.1534
878.5	0.4757	0.0882	0.1564
912.5	0.4730	0.0909	0.1612
934.5	0.4726	0.0913	0.1619
949.5	0.4728	0.0911	0.1616
960.0	0.4733	0.0906	0.1607
979.5	0.4724	0.0915	0.1623
1009.0	0.4721	0.0918	0.1628
1028.5	0.4709	0.0930	0.1649
1055.5	0.4682	0.0957	0.1697
1078.0	0.4688	0.0951	0.1686
1103.0	0.4669	0.0970	0.1720
1123.0	0.4668	0.0971	0.1722
1147.0	0.4665	0.0974	0.1727
1172.0	0.4648	0.0991	0.1757
1197.5	0.4633	0.1006	0.1784
1219.0	0.4624	0.1015	0.1800
1247.0	0.4613	0.1026	0.1819
1266.5	0.4608	0.1031	0.1828
1293.0	0.4591	0.1048	0.1858
1316.5	0.4592	0.1047	0.1857
1340.0	0.4586	0.1053	0.1867
1362.5	0.4582	0.1057	0.1874
1394.0	0.4556	0.1083	0.1921
1414.0	0.4545	0.1094	0.1940
1436.5	0.4557	0.1082	0.1919

Table B.7 Data for test at 275°C

Time	Sample Mass	Mass Loss	Normalized
0.0	0.7449	0.0000	0.0000
2.0	0.7445	0.0004	0.0004
5.0	0.7468	-0.0019	-0.0019
20.0	0.7299	0.0150	0.0150
23.0	0.7279	0.0170	0.0170
28.0	0.7223	0.0226	0.0226
43.0	0.7107	0.0342	0.0342
48.0	0.7071	0.0378	0.0378
73.0	0.6923	0.0526	0.0526
93.5	0.6851	0.0598	0.0598
103.0	0.6807	0.0642	0.0642
123.0	0.6740	0.0709	0.0709
140.0	0.6682	0.0767	0.0767
145.5	0.6643	0.0806	0.0806
168.0	0.6598	0.0851	0.0851
173.5	0.6593	0.0856	0.0856
192.0	0.6553	0.0896	0.0896
199.0	0.6518	0.0931	0.0931

Table B.8 Data for test at 300°C

Time	Sample Mass	Mass Loss	Normalized
0.0	0.6881	0.0000	0.0000
1.0	0.6901	-0.0020	-0.0029
2.0	0.6912	-0.0031	-0.0045
3.0	0.6901	-0.0020	-0.0029
4.0	0.6853	0.0028	0.0041
5.0	0.6845	0.0036	0.0052
6.0	0.6836	0.0045	0.0065
7.0	0.6832	0.0049	0.0071
8.0	0.6809	0.0072	0.0105
9.0	0.6796	0.0085	0.0124
10.0	0.6782	0.0099	0.0144
11.0	0.6771	0.0110	0.0160
12.0	0.6756	0.0125	0.0182
13.0	0.6746	0.0135	0.0196
23.0	0.6612	0.0269	0.0391
24.0	0.6599	0.0282	0.0410
25.0	0.6592	0.0289	0.0420
26.0	0.6586	0.0295	0.0429
50.0	0.6346	0.0535	0.0778
74.0	0.6196	0.0685	0.0995
91.0	0.6136	0.0745	0.1083
95.0	0.6106	0.0775	0.1126
98.0	0.6116	0.0765	0.1112
104.0	0.6071	0.0810	0.1177
116.0	0.6021	0.0860	0.1250
120.0	0.6011	0.0870	0.1264
124.0	0.6000	0.0881	0.1280
128.0	0.5976	0.0905	0.1315
141.0	0.5956	0.0925	0.1344
143.0	0.5946	0.0935	0.1359
146.0	0.5926	0.0955	0.1388
150.0	0.5906	0.0975	0.1417
164.0	0.5856	0.1025	0.1490
168.0	0.5849	0.1032	0.1500
172.0	0.5841	0.1040	0.1511
188.0	0.5806	0.1075	0.1562

REPORT DOCUMENTATION PAGE

Public reporting burden for this collection of information is estimated to average 1 hour per response, including the time for reviewing instructions, searching existing data sources, gathering and maintaining the data needed, and completing and reviewing the collection of information. Send comments regarding this burden estimate or any other aspect of this collection of information, including suggestions for reducing this burden, to Washington Headquarters Services, Directorate for Information Operations and Reports, 1215 Jefferson Davis Highway, Suite 1204, Arlington, VA 22202-4302, and to the Office of Management and Budget, Paperwork Reduction Project (0704-0188), Washington, DC 20503.

1. AGENCY USE ONLY (Leave blank)	2. REPORT DATE	3. REPORT TYPE AND DATES COVERED
	February 2000	Final Contractor Report

4. TITLE AND SUBTITLE

Long Term Degradation of Resin for High Temperature Composites

5. FUNDING NUMBERS

WU–714–04–40–00
NAS3–2054

6. AUTHOR(S)

Kaustubh A. Patekar

7. PERFORMING ORGANIZATION NAME(S) AND ADDRESS(ES)

Massachusetts Institute of Technology
77 Massachusetts Avenue
Cambridge, Massachusetts 02139–4307

8. PERFORMING ORGANIZATION REPORT NUMBER

E–12155

9. SPONSORING/MONITORING AGENCY NAME(S) AND ADDRESS(ES)

National Aeronautics and Space Administration
John H. Glenn Research Center at Lewis Field
Cleveland, Ohio 44135–3191

10. SPONSORING/MONITORING AGENCY REPORT NUMBER

NASA CR—2000-209918

11. SUPPLEMENTARY NOTES

12a. DISTRIBUTION/AVAILABILITY STATEMENT

Unclassified - Unlimited
Subject Category: 24   Distribution: Nonstandard

This publication is available from the NASA Center for AeroSpace Information, (301) 621–0390.

12b. DISTRIBUTION CODE

13. ABSTRACT (Maximum 200 words)

The durability of polymer matrix composites exposed to harsh environments is a major concern. Surface degradation and damage are observed in polyimide composites used in air at 125 to 300 °C. It is believed that diffusion of oxygen into the material and oxidative chemical reactions in the matrix are responsible. Previous work has characterized and modeled diffusion behavior, and thermogravimetric analyses (TGAs) have been carried out in nitrogen, air, and oxygen to provide quantitative information on thermal and oxidative reactions. However, the model developed using these data was not able to capture behavior seen in isothermal tests, especially those of long duration. A test program that focuses on lower temperatures and makes use of isothermal tests was undertaken to achieve a better understanding of the degradation reactions under use conditions. A new low-cost technique was developed to collect chemical degradation data for isothermal tests lasting over 200 hr in the temperature range 125 to 300 °C. Results indicate complex behavior not captured by the previous TGA tests, including the presence of weight-adding reactions. Weight gain reactions dominated in the 125 to 225 °C temperature range, while weight loss reactions dominated beyond 225 °C. The data obtained from isothermal tests was used to develop a new model of the material behavior. This model was able to fully capture the behavior seen in the tests up to 275 °C. Correlation of the current model with both isothermal data at 300 °C and high rate TGA test data is mediocre. At 300 °C and above, the reaction mechanisms appear to change. Attempts (which failed) to measure non-oxidative degradation indicate that oxidative reactions dominate the degradation at low temperatures. Based on this work, long term isothermal testing in an oxidative atmosphere is recommended for studying the degradation behavior of this class of materials.

14. SUBJECT TERMS

Composites; Fibers; Polymers; Durability; Mechanical properties

15. NUMBER OF PAGES

114

16. PRICE CODE

A06

17. SECURITY CLASSIFICATION OF REPORT	18. SECURITY CLASSIFICATION OF THIS PAGE	19. SECURITY CLASSIFICATION OF ABSTRACT	20. LIMITATION OF ABSTRACT
Unclassified	Unclassified	Unclassified	